January 2021

Deciphering The Effects Of Serelaxin On The Cardiorenal Axis In Acute Heart Failure- A Canine Model

Abhinav Chinna Krishnan
Wayne State University

DECIPHERING THE EFFECTS OF SERELAXIN ON THE CARDIORENAL AXIS IN ACUTE HEART FAILURE- A CANINE MODEL

by

ABHINAV KRISHNAN

DISSERTATION

Submitted to the Graduate School

of Wayne State University,

Detroit, Michigan

in partial fulfillment of the requirements

for the degree of

DOCTOR OF PHILOSOPHY

2021

MAJOR: PHYSIOLOGY

Approved By:

_____

Advisor Date

_____

_____

_____

_____

DEDICATION

This dissertation is dedicated to my wife, Jennifer, and my two beautiful kids, Kiran Asher and Riaan Jace. This has been a long journey for me, and I am confident, for you as well. There aren't words to describe the appreciation and admiration I have for you. Thank you for your unwavering support and endless love.

To my parents Murali and Latha Krishnan, you have always been my strongest fans and supporters, without whom none of this would have been possible.

To my sister Mithila Krishnan, thank you for always believing in me and keeping me smiling.

Finally, to my friends and lab mates, thank you for your understanding. All of this would not be possible without you.

ACKNOWLEDGEMENTS

I would like to first and foremost thank my advisor **Dr. Phillip D. Levy.** As you are aware, you are more than an advisor, mentor, and PI to me. With your natural ability to inspire, educate, and motivate those around you, it's easy to see what prompted me to follow and learn from you. You are one of the greatest examples of a leader I can think of. Thank you for changing my life and making my Ph.D. journey such a rewarding and exciting experience.

I would like to thank my committee members: **Dr. Karin Przyklenk**, thank you for teaching me how to conduct research effectively and appropriately. Your wisdom and guidance will always be revered. **Dr. Noreen F. Rossi**, this dissertation would never have come to fruition if you hadn't encouraged me to pursue it. Thank you for always having faith in me and your students. **Dr. Donal S. O'Leary**, thank you for giving me the opportunity to work in your lab and grow as a scientist under your supervision. **Dr. Joseph Dunbar**, thank you for agreeing to serve on my committee and for your unwavering guidance as I pursued this degree. **Dr. David Lanfear,** thank you all of your advice and for always giving me your time, no matter the short notice.

Dr. Javier Sala-Mercado, you first found me wandering the halls of the Elliman building reading physiology posters. After a short conversation, you bought me lunch and recruited me to work in the lab the following week. You are a role-model to all of the students who cross paths with you. Your passion and confidence are infectious, and I hope to one day emulate your qualities. **Dr. Marty Spranger**, **Dr. Jasdeep Kaur, Dr. Danielle Senador, Dr. Robert Hammond.** My lab-mates and mental health workers, we have been through much together. Thank you for spending a part of your lives with me.

Thank you for teaching me lab techniques, surgeries, how to perform experiments, analyze the results, and put everything together in a manuscript. Your time and support of my PhD candidacy, your advice/counsel, and your patience will always be remembered. **Audrey Nelson**, **Jody Helme-Day**, **Abe Lovelace**, **Alberto Alvarez, Kimberly Aung**, **Hanna Hanna**, **Peter Levanovich**, **Janine Mattei**, **Dr. Elizabeth Dawe, Dr. Gerald Hish**, and **Dr. Joseph T. Mannozzi** thank you for helping bring this study to life and for completing it. You all made coming to lab a vibrant, stimulating, and productive atmosphere. My profound gratitude to my work supervisors, **Parada Jordan** and **Jamie Krueger**. If it wasn't for the opportunities and understanding you provided, I would never have had the ability to take care of my family and pursue my dreams. A special thanks to my friends **Dr. Mohammad El-Chami, Bruce Linebaugh, and Vishnu Undyala,** for supporting me through the completion of this project, you are always remembered and appreciated.

Finally, and most importantly, **Christine Cupps**. My final thank you is to you. Words can't describe the appreciation I have for you in giving me your time, guidance, and support. Thank you for always being there for every step of the way for students in the Physiology program. You are a pillar in this school and certainly in my life.

TABLE OF CONTENTS

LIST OF TABLES

LIST OF FIGURES

LIST OF ABBREVIATIONS

ACS	Acute Coronary Syndrome
AF	Atrial Fibrillation
AHA	American Heart Association
ALK	Activin receptor-like kinase
ANOVA	Analysis of Variance
ARRIVE	Animal Research: Reporting of In Vivo Experiments
AVMA	American Veterinary Medical Association
BCS	Body Condition Score
BID	Bis in Die (Twice a day)
CAM	Coronary Artery Microembolization
CBF	Coronary Blood Flow
CO	Cardiac Output
CP	Cardiac Power
cTnI	Cardiac Troponin I
cTnT	Cardiac Troponin T
DOCA	Deoxycorticosterone acetate
DSI	Data Science Instrument
dp/dt_{MAX}	Contractility
dp/dt_{MIN}	Lusitropy
E_a	Arterial Elastance
EF	Ejection Fraction
FDA	Food and Drug Administration

FITC-Inulin	Fluoresceinyl Isothiocyanate-labeled-Inulin
Fr	French
GFR	Glomerular Filtration Rate
HF	Heart Failure
HFpEF	Heart Failure with Preserved Ejection Fraction
HFrEF	Heart Failure with Reduced Ejection Fraction
HR	Heart Rate
IACUC	Institutional Animal Care and Use Committee
ICM	Ischemic Cardiomyopathy
IV	Intravenous
LV	Left Ventricle
LVEDP	Left Ventricular End Diastolic Pressure
LVP	Left Ventricular Pressure
MAP	Mean Arterial Pressure
NYHA	New York Heart Association
NT-proBNP	N-terminal Pro B-Type Natriuretic Peptide
PO	By Mouth
RAAS	Renin-Angiotensin-Aldosterone-System
RBF	Renal Blood Flow
RVP	Rapid Ventricular Pacing
RXFP	Relaxin-Family Peptide
SLX	Serelaxin
SV	Stroke Volume

SDS-PAGE	SDS-polyacrylamide gel
TDD	Transdermal
TGF-β	Transforming growth factor-β

CHAPTER 1 - BACKGROUND ON ACUTE HEART FAILURE

Cardiovascular systems rely on the interplay between various complex mechanisms to maintain homeostasis [1]. However, in pathological states like heart failure, there is a shift from normal processes to compensatory extremes that often lead to negative consequences to various organ systems in terms of structure and function [2].

The American Heart Association (AHA) reports that from 2020 to 2021, heart failure (HF) remained the most significant contributor to mortality after the COVID-19 pandemic [3,4]. The burden acute HF poses to the healthcare system is substantial, with 6 million Americans diagnosed annually at the cost of $35 billion with projections it will double to a cost $70 billion, affecting nearly 8 million people by 2030 [3,5,6]. Despite this, outcomes for acute HF have not significantly improved in decades, prompting interest in novel therapeutics to alter this trajectory [7-12].

A diagnosis of acute HF is defined by either a new onset of symptoms or exacerbated symptoms induced by known underlying ischemic cardiomyopathy [13-15]. In patients with new, sudden symptoms, which comprise nearly 20% of all cases, they can occur by viral/drug agent, valvular dysfunction, or increased sympathoactivation, causing acute increases in filling pressures [16,17]. For patients with worsening symptoms of pre-existing HF, which comprise nearly 80% of all cases, it typically occurs due to precipitating factors like acute coronary syndrome (ACS), infection, atrial fibrillation (AF), hypertension, and non-compliance [17,18]. Accordingly, acute HF patients can be triaged into two groups: one with and the other without a history of HF. Physiological changes for acute HF patients include increased fluid retention (causing increased weight gain) as opposed to pulmonary edema [19-22], dysregulation of neuro-hormonal mechanisms that begin to progressively worsen causing further decompensation, and cardiogenic shock due to

decreased cardiac output [14,15,17,19,23]. Ultimately, acute HF with underlying ischemic heart disease can result from multiple sequelae that may lead to patients having other comorbidities strongly associated with adverse health outcomes and poor quality of life [19,24-27].

In acute HF, the diseased cardiac substrate can be associated with either systolic or diastolic dysfunction, which can also be better classified by ejection fraction (EF) as heart failure with reduced ejection fraction (HFrEF) or heart failure with preserved ejection fraction (HFpEF) [28,29]. Both HFrEF and HFpEF display symptoms of dyspnea/exercise intolerance, volume overload, and increased risk of mortality and low quality of life[13,21,24,30]. Due to the growth in the number of elderly individuals in the United States population over the last decade, there may be a shift in more patients diagnosed with HFpEF over HFrEF [31]. Nevertheless, HFrEF continues to present in most cases with higher in-hospital mortality, exaggerated RAAS activation, and an enlarged-hypertrophic left ventricle (LV) [32-35]. These factors expose the heart, kidney, and other end-target organs to ischemic-like conditions that may manifest to chronic HF.

For these reasons, ischemic heart disease is principal culprit in patients with a clinical diagnosis of chronic HF. Therefore, the etiology of acute HF is dependent on the degree of the pre-existing ischemic cardiomyopathy, which initiates various compensatory mechanisms that causes inflammation, fibrosis production, and cardiac remodeling [36,37]. These remodeling processes though initially beneficial, become progressively aberrant and uncoordinated, which if not managed becomes maladaptive to both cardiac structure and function as well as end-organ damage [38,39]. During this critical condition, an acute precipitant, like exercise, may shift this balance and cause decompensation and ischemia [40,41]. The overall mechanistic pathways attenuated and

exaggerated in acute HF are shown in the adapted Figure 1.1 from Freda and Slawsky, 2011 [23].

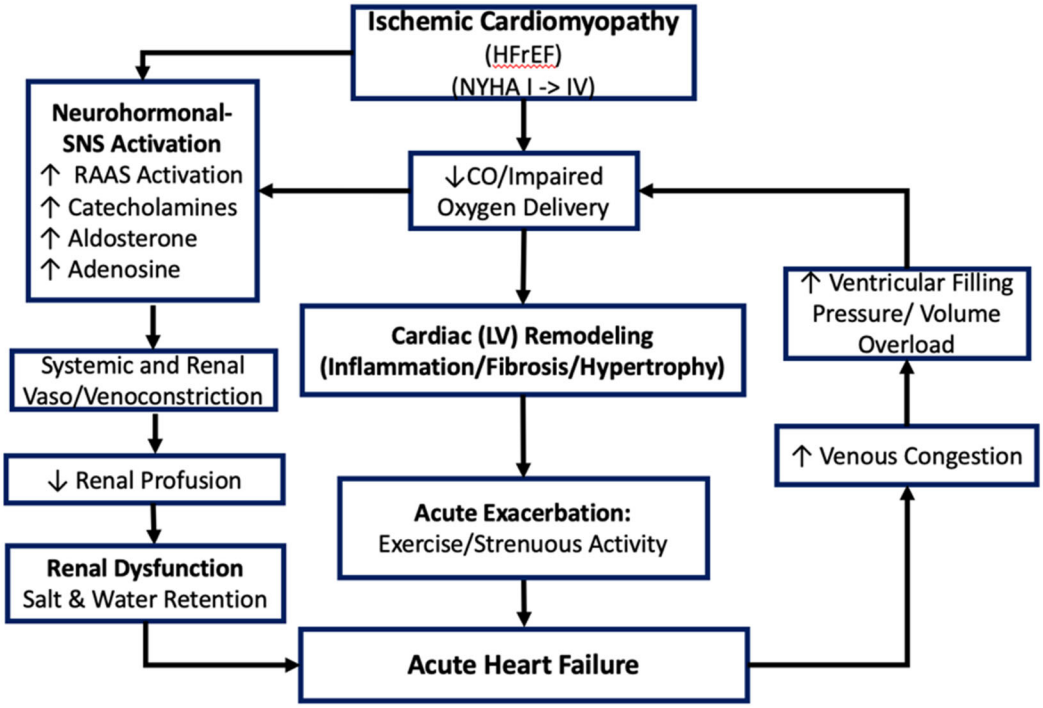

Figure 1.1: The pathophysiology of acute HF with underlying ischemic cardiomyopathy. Cardiac output (CO), Renin-Angiotensin-Aldosterone-System (RAAS), Left Ventricle (LV), New York Heart Association (NYHA), Heart failure with reduced ejection fraction (HFrEF), sympathetic nervous system (SNS). Adapted from Freda and Slawsky, 2011 [23].

The overall goal of treatment for acute HF is to mitigate symptoms but also ideally to prevent/reverse cardiac remodeling which is typically in late-phase conditions [42]. During remodeling, there are alterations to the ventricle in terms of size, function, and shape due to neurohormonal, mechanical, and genetic factors [39,43,44]. Within a few hours following a cardiac insult (i.e., myocardial infarction) begins the early phase of ventricular remodeling [36-38,43,45-47]. To maintain stroke volume (SV) and cardiac output (CO), there is exaggerated sympathetic activation that releases catecholamines to vasoconstrict the systemic vasculature and maintain CO [44]. Due to myocardial scarring, there is an impact on contractility due to the necrotic tissue and the decrease in the number of contractile

units in the myocardium, which forces the ventricle to create increased pressure against a higher afterload [35-37,42,44-46]. During the middle phase, measured in hours to days, there is an effort to repair damaged tissue [35,48]. Therefore, collagen forming activators are recruited to replace the necrotic tissue in the scar as well as an increase in transforming growth factor-β (TGF-β) associated pathways, which are able to promote apoptosis and hypertrophy by inhibiting the activin receptor-like kinase (ALK) & SMAD pathways [49-51]. Finally, during late-phase remodeling, occurring from days to weeks, there is a stabilization of wall stress; however, the compensatory mechanisms begin to run away and do not terminate, and as such would be an ideal therapeutic target [46,52]. Interestingly, recent evidence suggests that long-term treatment of HF by neurohormonal blocks in particular (i.e., renin/aldosterone blockers) to mitigate symptoms has been shown to in fact increase negative-remodeling processes [48]. In summary, the goal of HF management is treatment within a few hours of presentation and to prevent the downstream cascade of remodeling as seen above [43,46,47].

Clinical assessment of acute HF is by profusion (hot or cold) or by congestion (wet or dry) evaluation [17,53]. Gold-standard markers of acute HF involves natriuretic peptides, troponin, hemodynamics, and assessment of renal function and electrolytes [17]. Unfortunately, as previously stated, many of the current therapeutics manage symptoms rather than reverse pathology [54]. Accordingly, pivotal trials of novel therapeutics to treat acute HF have largely failed and have not taken this to account [7,8,32,55].

CHAPTER 2 - TREATING ACUTE HEART FAILURE WITH SERELAXIN

Of the therapeutic agents studied to date that treat acute HF, none have proven to be efficacious in reversing its detrimental effects [10,35,47,55-61]. Serelaxin (SLX) (RLX 030, Novartis), a recombinant form of the human peptide relaxin-2 [9,54,62-64], initially showed promising results towards improving mortality and possibly impacting the pathophysiological effects of acute HF [8,54,62,65,66]. However, it was unsuccessful in Phase III trials [26,56,60,67]. Review of SLX in a translatable animal model may yet provide further insight into its mechanics in treating acute HF [68-72].

Relaxin was first identified in the early 1900s by Dr. Fredrick Hisaw during his study of pregnancy in guinea pigs [73]. It wasn't until later half of the 1900s where investigation by Dschietzig et al. into the effects of relaxin opened the possibility of whether the hormone could treat cardiovascular disease, specifically acute HF [65,74]. SLX is the recombinant form of the naturally occurring human hormone relaxin 2, secreted during pregnancy [65,75]. SLX's novelty for treating acute HF stems from its inherent ability to vasodilate the vasculature [10,75-78]. SLX was named to describe the role it plays in parturition whereby it "relaxes" the cervix; this mechanism of action also mediates cardiovascular responses such increasing cardiorenal hemodynamics, vascular compliance, and likely arterial elastance [9,62,65,75,79,80].

SLX belongs to a family of seven peptides that are involved in various metabolic and vasomotor regulatory activities while also possessing anti-fibrotic it has a desirable profile for therapeutic use in patients with acute HF [81-83]. The relaxin family peptide (RXFP) receptor is a G-protein coupled receptor that regulates the actions of SLX on the cardiovascular system vasodilating blood vessels, thereby increasing CO and renal blood flow (RBF) [84]. Further, SLX has also been reported to increase nitric oxide synthase and

impact late phase cardiac remodeling in heart failure by mediating the transforming growth factor-β/vascular endothelial growth factor pathways, matrix metalloproteinases, as well as the extracellular matrix of the vasculature [9,10,50,76,82,84-86]. Moreover, SLX also suppresses COX-associated inflammatory pathways [57,78]. Pharmacokinetic studies measuring half-life (6-8 hrs in humans) and bioavailability show rapid clearance (1-4 hrs) from the kidney and liver, following infusion of SLX intravenously (IV) [78,86-88].

In comparison with drug development for chronic HF, drug development for acute HF has been sparse with current treatment involving the use of diuretics and vasodilators (such as nitroprusside). Since the 1980's only a few drugs have been approved by the food and drug administration (FDA) for IV use in treating acute HF, for example, milrinone, levosimendan, and nesiritide [54,66]. For these reasons, SLX proved to be of interest due its physiological actions and its promising preliminary data regarding its reduction of mortality associated with acute HF [87,89-91]. One study from 2014 even postulated how long-term treatment, in parallel with the phases of cardiac remodeling as shown in Figure 2.1, may improve compensatory mechanisms acutely and attenuate negative processes chronically [92]. The utility of SLX seemed to have wide applicability, thus in addition to investigation of its role in treating heart failure, it has also shown impactful results in treating pathologies such as altered cerebral blood flow during hypoxia, hypertension, chronic kidney disease, and sclerosis [61,93,94].

Results from the pre-clinical trials matched SLX with favorable outcomes [51,54,66,74,77,89,90,95-97]. Key findings from the RELAX-AHF trial reported that of the 1161 patients enrolled, SLX treatment conferred dyspnea relief and reduction in mortality over 180-days [54]. Further, SLX also showed improvement in biomarkers like troponin, NT-proBNP, as well as Cystatin-C [92]. Yet, similar to previous acute HF drug studies, there

was no change for readmission/hospitalization following SLX treatment [19,26,65] and was subsequently rejected by the FDA and a European regulator. To explore SLX treatment in lieu of its impact in improving biomarkers of HF like troponin, a phase III study termed RELAX-AHF 2 was initiated to confirm whether SLX significantly reduced HF-associated biomarkers, death, and/or worsening HF outcomes post-5 days from treatment [56,58,60,67]. However, the definitive trial, which involved more than 6500 randomized subjects, reported neutral effects in terms of mortality benefit and associated hemodynamics/biomarkers [60,67,98]. Therefore, SLX was shown not to be effective as a first-line treatment for acute HF [26,56]. Model systems are always used to understand the basic pharmacology and pathways involved in a potential therapeutic, but all animal models are imperfect reflections of human pathophysiology, potentially leading to the inaccurate determination of true therapeutic effects [20,40,99]. Therefore, careful investigation in animal models that more closely resemble human disease could provide greater insights[68,72].

Understanding why drugs, like SLX, succeed or not is vital for future developmental efforts [8,21,41]. Yet animal models upon which drugs are developed do not typically reflect the varying presentations of acute HF, leading to potentially inaccurate determination of actual therapeutic effects [20,40,99]. In addition, many preclinical studies collect data during an anesthetized state, potentially confounding data [85,97,100].

With this in mind, we studied SLX using a canine model specifically tailored to reflect acute on chronic HF that recapitulates the many aspects of common human pathophysiology, including chronic ischemic etiology with decompensation due to an acute precipitant [41,56,101,102]. Importantly, this model utilizes non-anesthetized data collection in the conscious state allowing for unaltered determination of the hemodynamic

impact of specific drugs during an episode of acute decompensation [5,103-105]. This dissertation investigates the extent to which SLX impacts cardiac and renal hemodynamics in acute HF [21].

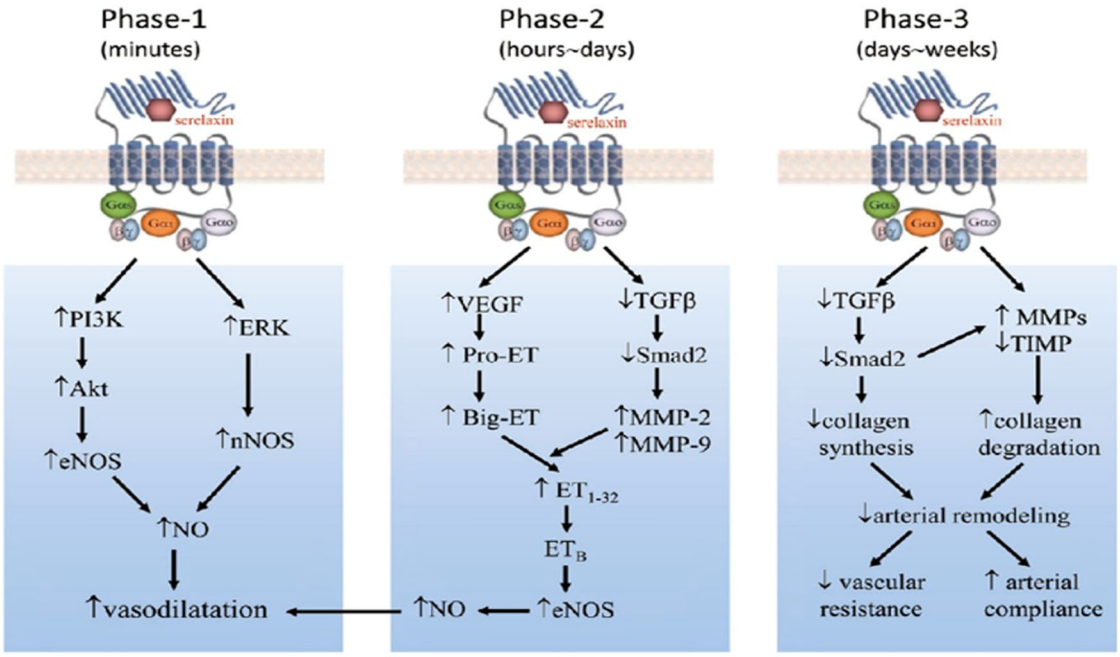

Figure 2.1: 3-phase time course of physiologic changes associated with serelaxin infusion. This time course reviews the mechanism of action of serelaxin (SLX) during the early, middle, and late phase shown as Phase 1, Phase 2, and Phase 3, respectively. SLX binding to the transmembrane RXFP receptor is shown above and post-intervention associated pathways below. This image was reported by Du et al., 2014[92]

SPECIFIC AIM: To determine if SLX infusion positively impacts the on-treatment effects of SLX infusion (vs. placebo) following acute HF on cardiac and renal function using hemodynamics, biomarker, and renal clearance.

i) I hypothesize that SLX infusion will recover the loss of function observed following acute HF-induced impact to cardiac hemodynamics versus control. Furthermore, that effective arterial elastance and cardiac-specific biomarkers will also significantly improve following SLX treatment.

ii) I hypothesize that the acute HF-associated impairment on renal hemodynamics and function will improve following SLX infusion.

CHAPTER 3 – DEVELOPMENT OF A TRANSLATIONAL CANINE MODEL OF ACUTE HEART FAILURE TO TEST EMERGING THERAPEUTICS

ABSTRACT

Many well-established large animal models of HF closely mirrors human pathophysiology. However, all face limitations and none are currently well-accepted for acute HF. Given the paucity of established models of acute decompensation, an aspect of HF that has gained increased attention over the past decade, translatable animal models are needed that evaluate its pathophysiology for drug development and scientific understanding. Herein we briefly review existing large animal models of HF and then describe a novel approach to invoke acute HF in canines. This model combines the state of chronic ischemic cardiomyopathy via coronary artery microembolization (CAM) with subsequent hemodynamic challenge using rapid ventricular pacing (RVP), thus enabling a recapitulation of clinical mechanisms that trigger decompensation. N-terminal pro B-type natriuretic peptide (NT-proBNP) and EF are used as function indicators of the methodology presented. Our translational CAM/RVP model could allow for better-targeted evaluation of therapeutics meant to lower the morbidity and mortality associated with HF by allowing better interrogation of this vulnerable period and specific acute stressors.

INTRODUCTION

Chronic HF is a major public health concern that affects over six million Americans [3,4,6] many of whom will experience periods of acute decompensation referred to as acute HF [16,22]. Episodes of acute exacerbation result in approximately one million associated hospitalizations annually, and remains the leading cause of hospital admission for patients age 65 years and older [15]. This leads to a decreased quality of life for patients

admitted and discharged from the hospital with acute HF as well as a large economic burden on the healthcare system [106,107].

Though definitive diagnosis is still challenging, components of evaluation for those with acute HF include dyspnea measures, blood pressure, fluid volume assessment, natriuretic peptides, and EF [13,27,52]. Cases in patients stem from idiopathic causes, neurohormonal activation or via cardiorenal dysfunction [14,108]. Worsening myocardial structure and function are not prerequisites for acute decompensation [14]. However, given that ischemic heart disease is one of the leading causes of death in the United States and with at least 53% of acute HF cases involving HFrEF, it is important to study models that incorporate this phenotype [3,4,14,24].

Acute HF is a prevalent condition that places great strain on patients and the healthcare system alike [15]. To improve upon this, novel approaches and therapeutics are needed [59,69]. Standardized and highly translational large animal models can facilitate the developmental process and provide insight into cardiorenal physiological responses [72]. However, to be most effective, these models must accurately represent acute HF phenotypes and recapitulate the human condition [109-113].

The purpose of this chapter is to: 1) provide a brief overview of current large animal models of acute HF and chronic ischemic cardiomyopathy (ICM), including circumstances when these models are most appropriate to employ, and 2) present a newly developed canine model that superimposes a tachycardic precipitant on underlying ischemic cardiomyopathy resulting in acute decompensation to test my hypotheses. Throughout, we will provide insight into developmental difficulties of our new model so that future researchers can build upon existing knowledge and avoid potential complications.

Current large animal models of chronic HF

There are several established models for the study of ICM in large animals. CAM, coronary ligation, RVP, volume overload, myocardial toxicity, and ischemia reperfusion are all well-recognized methods for inducing ischemic cardiomyopathy [69,72,109-111,113]. These models have been applied in canines, rabbits, pigs, and sheep. While other more extensive reviews of such models have been written, this manuscript focuses exclusively on canine models of ischemic cardiomyopathy that may be most applicable to the study of acute HF [72].

Ischemic models

Coronary ligation – ischemia-reperfusion

The coronary ligation model creates a reproducible ICM phenotype with a suture occlusion procedure [72,113]. Advantages include the ability to precisely control blood flow, allowing for ischemia-reperfusion studies, rapid preparation, and neurohormonal activation [91,101,113]. Disadvantages include the incidence of fatal arrhythmias, requirement for surgical skill and knowledge, inconsistent infarct size due to collateral circulation [114,115], and scar tissue development that prevents future surgical procedures [69,110,111,113]. Despite such considerations, models of ischemia and ischemia-reperfusion achieved by coronary ligation remains a valuable method for the study of infarct development, contractility changes in under-perfused tissue, myocardial remodeling, and cardioprotective agents [69,101,110].

Coronary artery microembolization

Initial embolization studies established a preparation for more diffuse cardiac damage than complete coronary ligation [116]. To enable more controlled, smaller infarcts, CAM was developed, with the injection of starch granules into specific branches of the

coronary circulation [116]. The CAM model has been gradually refined [72,117-120] and is considered a gold standard technique for the induction of ischemia, offering the benefits of non-reversible myocardial damage and the generation of a permanent ICM phenotype with high clinical correlation [110,121]. In addition, this approach allows for reliable targeting of a specific ejection fraction and controlled induction of a global ICM. Also, unlike coronary ligation methods, embolizations are performed via a minimally invasive, closed-chest preparation. CAM successfully produces inflammatory responses [122], LV dilation, increases in filling pressures, systolic and diastolic dysfunction, and myocardial scarring[123]. The downfalls of CAM include dispersed infarction areas, expensive preparation with a need for repeated procedures, dysrhythmias, and high mortality rates [69,110,113], along with the inability, in some models (i.e., canines), to achieve a sustained impairment in blood flow due to the development of coronary collateral circulation [124].

Non-ischemic models

RVP

Initial investigation of RVP created a reproducible HF preparation that avoided surgical trauma, ischemia, and toxic side effects of existing models (i.e., β-adrenergic dysfunction during the induction of canine cobalt cardiomyopathy) [125,126]. Subsequently, a reliable protocol for RVP was successfully developed [127-130] and is frequently used in large animal research [131]. Unlike some ischemic models, RVP generates chronic HF with a dilated ICM [110,124]. While this model succeeds in producing left or right ventricular dysfunction and neurohormonal alterations, it fails to produce permanent HF and ischemia-related damage as the HF animal often recovers after pacing is ceased [110,112,124,132]. However, more aggressive models, with increased frequency or duration of pacing, can be used to produce permanent underlying damage such as fibrosis,

hypertrophy, and increased filling pressures with preserved hemodynamics [127]. The model is technically easier to perform and utilizes less time and resources than ischemic models [69,113]. Furthermore, pacing is valuable in translational studies because it is highly reproducible [112]. This model is well suited for the furthering the study of the neurohormonal pathway, cardiac remodeling, and vascular changes during the onset or recovery from dilated ICM [69,110,124].

Pressure overload

The classic canine pressure overload model involves aortic banding (transverse aortic constriction) [133]. This model is advantageous for producing increases in LV hypertrophy, fibrosis, and stiffness of the ventricle [69,134]. Disadvantages include surgical preparation [134] and the prolonged time (8+ weeks) necessary for development of LV hypertrophy and remodeling [69,113]. Pressure overload is specifically well-suited for studying diastolic dysfunction in ischemic cardiomyopathy produced by underlying hypertrophy [69,113]. Aortic banding is similar to hypertension as it generates increases in afterload and produces comparable cardiac dysfunction and remodeling [133].

Hypertensive heart disease

While aortic banding does produce increased afterload, it does not result in changes in systemic blood pressure [110,133]. Other preparations do exist that more accurately generate hypertensive physiological changes, including occlusion or ligation of the renal artery [72]. Advantages of this model include sustained increases in blood pressure, neurohormonal activation, end-organ damage, and cardiac hypertrophy, among others [72,135]. Disadvantages include the development of renal collateral circulation within 2-3 months [135]. Similar preparations that wrap the kidney in silk with contralateral nephrectomy produce hypertension and LV hypertrophy [136]. Endocrine

induction of hypertension also exists by administering mineralocorticoids, such as deoxycorticosterone acetate (DOCA), paired with renal mass removal and a high salt diet [135,137]. This model also increases fluid volume, increased cardiac mass, and decreased kidney function [135]. Small animal models of genetically induced hypertension may be applicable in the future, but genetic manipulation has yet to be translated into large animal designs [137]. Unfortunately, hypertension-induced HF methods are rarely used in large animal models due to confounding factors such as cost or genetic variability [135]. Large animal models have been developed that establish HF followed by induction of acute hypertension, such as RVP followed by infusion of angiotensin II [138] or CAM with pacing and methoxamine pressure loading that are more time and cost appropriate [123]. However, there are few, if any, large animal models of HF with underlying hypertension and adequate clinical translatability.

Volume overload

There are several available pathways for the induction of ICM via volume overload, the most prominent being destruction of the mitral valve with induction of mitral regurgitation [69,110,113,124]. Advantages of mitral regurgitation include the use of a closed chest preparation, the accompanying neurohormonal activation, LV dilation and hypertrophy, and high clinical translatability for the volume overload HF phenotype [69,110,113,124]. Disadvantages include the approximate 3-month period before hypertrophy and dilation develop, as well as the lack of ischemic injury [110,113,124]. Both volume and pressure overload could be paired with other models of ICM to better represent what is seen clinically [110], but this has not yet been successfully developed to our knowledge.

Myocardial toxicity

Injection of toxic chemotherapeutic agents such as doxorubicin have proven to be

successful for induction of ICM [110,113,139-141]. Though less popular, this approach is advantageous due to its closed chest preparation [113]. Disadvantages include systemic side effects and high rates of arrhythmia [110,113]. Administration of the toxin often involves either repeated low-doses or one high-dose bolus, that could lead to exacerbated cardiotoxicity if dose-response curves are not properly observed. Systemic side effects can be reduced by sequential intracoronary administration [140,141]; however, this increases cost dramatically [110].

Development of a novel acute-on-chronic HF model

Despite a rich history of ICM model development, few models have been developed to specifically evaluate acute HF as mentioned in Chapter 1. Acute coronary artery occlusion can produce acute HF [142,143], but is accompanied by an excessive risk of mortality [142], and would perhaps not be as representative of acute HF than acute myocardial infarction. Volume overload by administration of colloid fluid has been shown to produce acute episodes of HF in the presence of underlying cardiac dysfunction [110,113] but the responses are inconsistent and dependent on concurrent renal function. Acute hypertensive HF using pharmaceuticals to induce increased afterload has also been used with varied success [123] but, absent underlying cardiomyopathy do not reliably induce an acute decompensated state. Moreover, a recent review of existing HF animal models concluded that HF is caused by myriad disorders stating that the model selected must closely match the type of HF being studied, that no one comprehensive model of HF exists, and that combinations of existing acute and chronic models are needed [110]. Critical to the entire discussion is the duality of processes, which necessitates both an acute precipitant and underlying heart disease

In their review, Monnet et al [110] specifically suggest the value of a model pairing

an ischemic preparation with acute pacing to help understand clinical HF and therapeutic strategies. Atrial arrhythmias are a common cause of decompensation in patients with ICM [144] and a model combining the chronic ICM state with short-term pacing induced tachycardia has clinical relevance. Using the combined expertise of two established large animal labs, we designed such a model [40,145,146]. Our novel model closely adheres to recommendations set by the AHA as well as the American College of Cardiology and the European Society of Cardiology on how a model of dilated cardiomyopathy should be structured, measured, and analyzed, [109,147] and has broad applicability to the study of other novel therapeutics. Figure 3.1 provides an overview of model development with specific details on the successful implementation on 10 canines, including the overall process and procedures.

METHODS

Experimental subjects

Ten mixed-bred mongrel canines (6 females, 4 males; 21-27 kg; 8-10 months old) were chronically instrumented for hemodynamic measurements (Figure 3.3, Adobe Illustrator, CS5). All animals were acclimatized to the laboratory surroundings and trained to stand quietly in a sling for rest data via positive reinforcement. Canines were sourced from Marshall Bioresources and fed a standard Purina puppy chow diet based on their body score index assessed by veterinary guidance and were given free access to water. Procedures performed began between 07:00-10:00 hrs., in fluorescent-lit rooms with a controlled temperature between 23-25° C. Canine kennels operated with a 12-hour day/night cycle. Inclusion criteria included mixed-bred canines, 21-27 kg, 8-10 months of age. As this was a model development study there were no a priori exclusion criteria other than extreme illness in the animals and there was no blinding of results. All the procedures

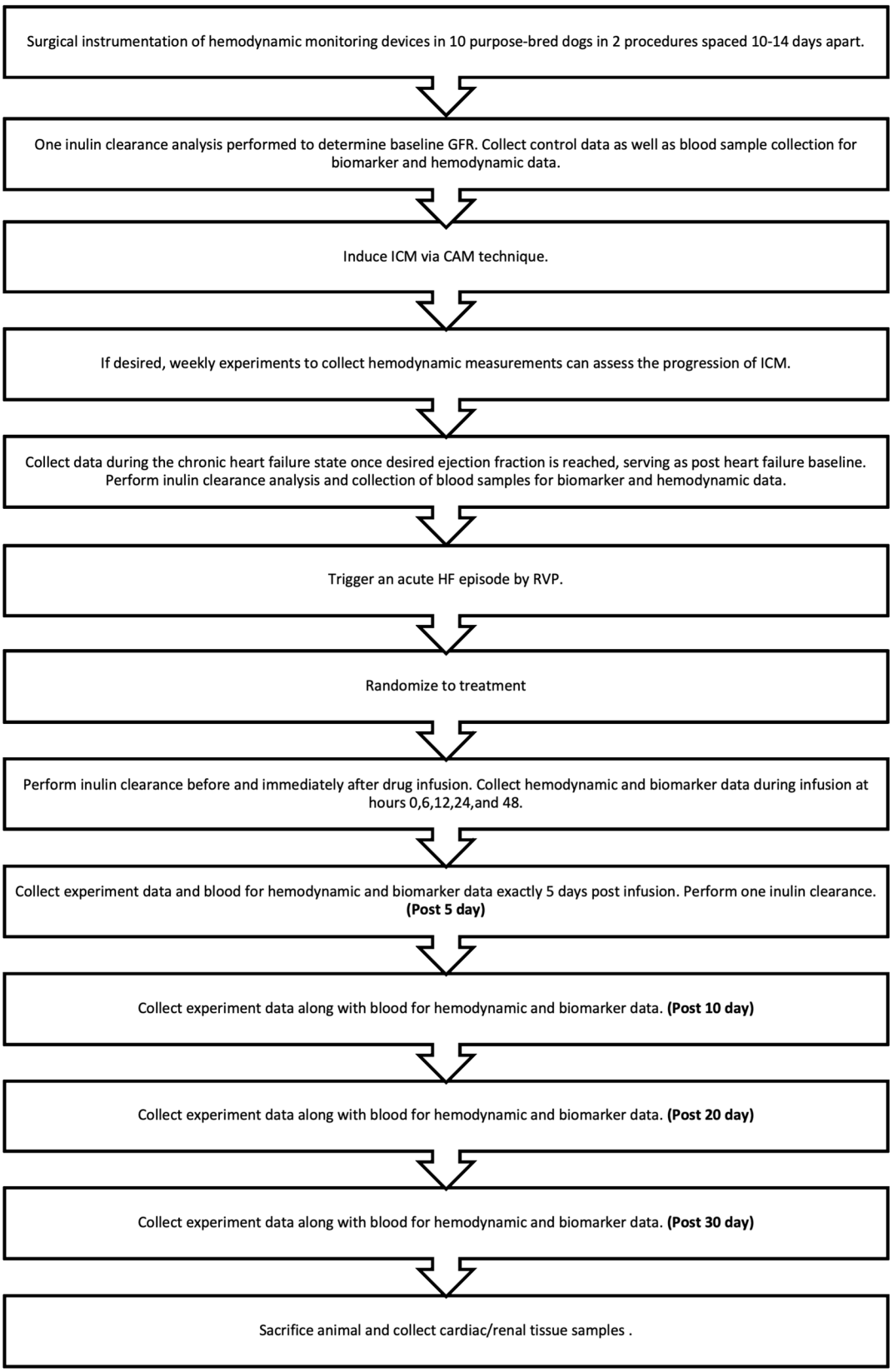

Figure 3.1: Protocol overview. Outline of the important steps in the acute HF study protocol over time. See text for definition of abbreviations.

were approved by the Institutional Animal Care and Use Committee (IACUC) of Wayne State University, complied with the National Institutes of Health Guide to the Care and Use of Laboratory Animals, and performed in accordance with relevant guidelines and regulations. Reporting in the manuscript follows the recommendations in the Animal Research: Reporting of *In Vivo* Experiments (ARRIVE) guidelines.

Surgical instrumentation and procedures

Preparation

In preparation for surgical instrumentation, animals were pre-anesthetized via an intramuscular injection of buprenorphine (0.01-0.03 mg/kg) and acepromazine (0.02-0.05 mg/kg). Once sedated, a combined mixture of ketamine and diazepam (5 mg/kg and 0.2-0.3 mg/kg IV, respectively) was administered prior to endotracheal intubation. Preoperative administration of carprofen (4.4 mg/kg IV) and a transdermal fentanyl patch

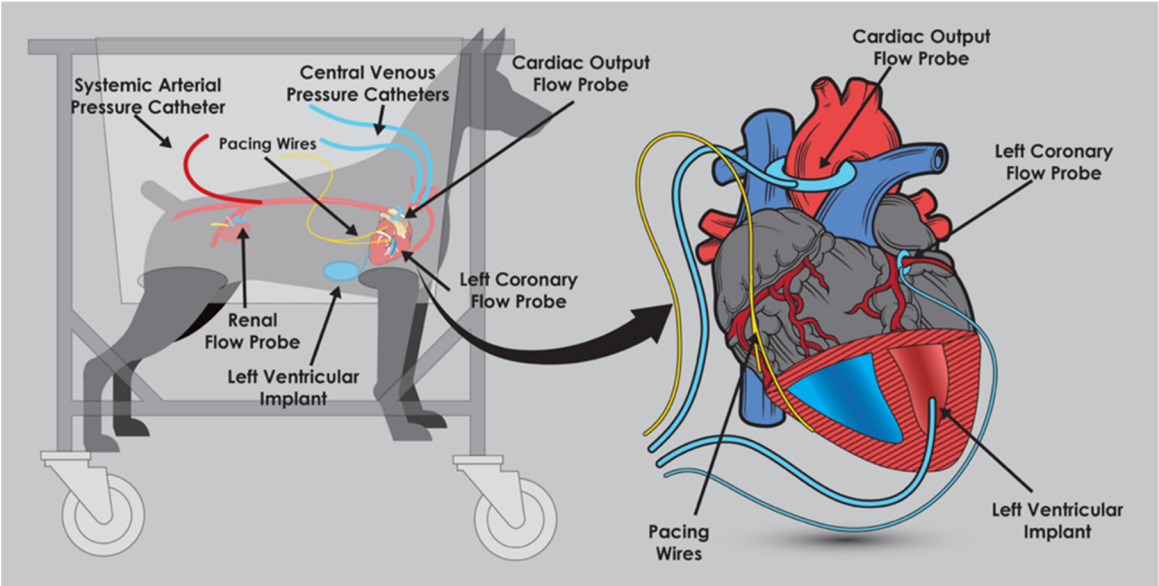

Figure 3.2: Visual representation of canine Instrumentation. Illustration of canine instrumentation used in the study protocol. Canine in the sling, full view of catheter, flow probe, LV implant and pacing wire placement (Left). Enlarged view of flow probe and pacing wire placement on the heart and surrounding vasculature (Right). See text for definition of abbreviations.

(50-125 μg/h TDD) were also given over 72 hours. Anesthesia was maintained pre/intraoperatively with isoflurane gas (1-3%). Animals were carefully monitored post-operatively and given buprenorphine and acepromazine subcutaneously (0.01-0.03 mg/kg and 0.2-0.3 mg/kg) as needed, thus ensuring multimodal anesthetic/analgesic care. Furthermore, canines received IV antibiotics (cefazolin 1g/1mL) before and after surgery and were continued prophylactically (cephalexin 500 mg, BID) thereafter by oral delivery for the duration of the experimental protocol.

Thoracotomy

In the first surgical procedure a left thoracotomy was performed through an incision at the 3rd or 4th intercostal space. A telemetry pressure transmitter (TA11 PA-D70, Data Sciences International) was implanted subcutaneously two intercostal spaces caudal to the thoracotomy incision. The implant was secured at the level of the left ventricular apex though a 5-7 cm incision, and its catheter tunneled into the thorax at the 7th intercostal space. An incision was then made to the pericardium to expose the heart. Following a puncture into the apex of the heart the catheter was then inserted and sutured in place with 4-0 prolene to measure left ventricular pressure (LVP). A perivascular flow probe (3PSB, Transonic Systems) was placed around the circumflex coronary artery to measure coronary blood flow (CBF). Four stainless steel ventricular pacing electrodes (0-Flexon, Ethicon) were secured to the right ventricular free wall. In addition, for measurement of CO, a perivascular flow probe (20PAU, Transonic Systems) was placed around the ascending aorta. Finally, the pericardium was loosely reapproximated, avoiding the phrenic nerve and the left anterior descending coronary artery. All wires were then made to exit the thorax through the 4th or 6th intercostal space and then tunneled subcutaneously and exteriorized between the scapulae at the dorsal midline through a

0.5-1.0 cm incision. After at least ten days of recovery, a second surgical procedure was performed.

Retroperitoneal

In the second surgical procedure, via a left flank retroperitoneal approach, additional flow and pressure measuring devices were implanted using the same surgical preparation as described above. A perivascular flow probe (4PSB, Transonic Systems) was placed around the left renal artery to measure RBF. In addition, a single 19-gauge polyvinyl catheter (Tygon, S54-HL, Norton) was inserted into a branch of the terminal aorta and advanced cranially approximately 15 cm to measure systemic mean arterial pressure (MAP) and for blood collection. The transducer cable and catheter were tunneled subcutaneously and exteriorized between the scapulae on the dorsal midline via a 0.5-1 cm incision next to the incision from the previous surgery, and all incisions were closed in layers. The animals were allowed 10 days to recover before any additional procedures were conducted. After recovery, baseline hemodynamic data and renal function were assessed.

Data acquisition

To collect hemodynamic data, indwelling catheters were connected to pressure transducers set at mid-heart level and MAP was measured. Perivascular probes were connected to flow meters to measure CO, CBF, and RBF. A telemetry transducer was used to measure LV pressure. All data were collected standing at rest on the treadmill or a sling. Hemodynamic data were recorded continuously on a computerized data acquisition system at 1000 Hz for subsequent analysis as beat-by-beat averages and as raw waveforms. Advanced hemodynamic calculations such as LVEDP were made using LabScribe 3 software (iWorx, Dover, NH).

Biomarkers

To collect blood samples for biomarker analysis, indwelling catheters were aspirated. Plasma concentrations of NT-proBNP were quantified using a commercially available canine-specific ELISA kit (Kamiya Biochemical Company, Seattle WA, catalog # KT-23770) as per the manufacturer's instructions. A 96-well plate reader was used to measure the results.

Inulin clearance

In addition to RBF, renal function was assessed by inulin clearance using an established protocol [148]. Given the 4-hour duration of the procedure a lactated ringer solution was infused IV at a rate of 3 ml/kg/hr from 30 min prior to the beginning of the clearance experiment and continued throughout the duration of the procedure. Animals were anesthetized for the sterile foley catheter (8-10 Fr) insertion using propofol (3-6 mg/kg) and maintained on sevoflurane (2-5%) with 100% oxygen in effort to minimize the vasodilatory effect of the anesthetics on inulin measures. Total time under anesthesia was less than 20 min. Upon consciousness, fluorescein isothiocyanate-labeled inulin (FITC-inulin, Sigma Aldrich) was administered via an indwelling venous catheter using a bolus injection of 5 mg/kg IV in 10 ml isotonic saline over 1 min followed by constant infusion at 0.25 mg/kg/min delivered in 0.35 ml/min isotonic saline via an infusion pump (3D Mini, SAI infusion technologies). After an equilibration period of one hour, the collection bag was emptied of urine. Then, three 30-minute urine collections were obtained as described previously [149,150]. As required for accurate inulin clearance analysis, 100% of urine output was collected after catheterization using a closed urine collection system. At the midpoint of each clearance period, whole blood was obtained via the indwelling arterial catheter for measurement of plasma inulin concentration. The

volume of urine was measured gravimetrically. Blood and urine samples were processed immediately after following the conclusion of the clearance procedure for that day. FITC-inulin fluorescence in plasma and urine samples was measured using a plate reader with excitation and emission wavelength of 490 and 520 nm, respectively [149]. Plasma and urine samples were assessed for sodium and potassium by flame photometry. All samples were analyzed at least in duplicate.

Microembolization (induction of ischemic cardiomyopathy)

In the third surgical procedure, animals were pre-medicated before each CAM with hydromorphone (0.1 mg/kg) and acepromazine (0.02-0.05 mg/kg) and received pre-and post-operative doses of cefazolin (1g/1mL). All animals were maintained intraoperatively with isoflurane (1-1.5%). On the ventral side of either the right or left hindlimb, the femoral artery was nicked, and a sheath was placed. Using fluoroscopic guidance, a catheter was advanced into the heart via the sheath. Bolus injections consisted of a solution of deionized water (1-5 mL) that contained approximately 2.5% polystyrene latex microspheres by volume (Polysciences, Warrington, PA, 4-5×104 particles/1 mL), with each particle ~90 μm in diameter. Microspheres were warmed to room temperature and, once vortexed, were subsequently injected within 5-10 sec. Injections were repeated incrementally until vitals and function showed impairment (i.e., ST-segment elevation, supraventricular tachycardia, and decreased ventricular wall motion) but before adverse outcomes. Microspheres were injected sub-selectively in an alternating fashion into the circumflex and left anterior descending coronary arteries. Microembolizations were repeated weekly until the EF reached our a priori targeted value of 30-40%. The animals underwent 5-20 intracoronary embolizations to produce this level of cardiac dysfunction. The procedure was performed on alternating legs each week.

Before the CAM, a ventriculogram and/or ultrasound was captured to measure baseline EF qualitatively. Subsequent determinations for EF with videos were captured using a 15 fps OEM c-arm fluoroscopy machine with a vascular package and were measured against EF obtained using a GE Vivid-I portable ultrasound machine in real-time. During and following the CAM, vitals were carefully monitored using the implanted instrumentation, pulse oximetry, and ultrasound, especially for pre-ventricular contractions, heart and respiratory rate increases, and drops blood oxygenation (SPO2); propranolol (10 mg PO) and buprenorphine (0.01 mg/kg IV) were given as needed. The canines were allowed at least one week to recover before another CAM procedure was performed. Upon achievement of the targeted EF, hemodynamic data and renal function were reassessed.

Rapid ventricular pacing (induction of acute HF)

Following induction of ischemic cardiomyopathy, angiography was repeated and if the EF remained < 40%, an RVP protocol was employed to induce acute HF. Pacing electrodes implanted in the first surgery were connected to an external pacer. During the initial pacing period, the heart rate was set at ~180 bpm and then progressively increased to a maximum of ~240 bpm. The rate was titrated based on hemodynamics and the animal's overall health status. Hemodynamics and symptoms of acute HF including pulmonary edema, dyspnea, and lethargy, were checked multiple times daily. Animals were paced for a period of 1-21 days to achieve the target degree of acute HF as described below.

Our intent was not to induce florid pulmonary edema as this is often unrecoverable in canine models once present. Instead, we targeted hemodynamic evidence of acute decompensation, with an initial goal to increase LV end-diastolic pressure (LVEDP) by

50%. However, we found that we were unable to reliably achieve this goal, as shown in Table 3.1, presumably because the animals were mainly in a compensated, euvolemic state of cardiac dysfunction.

Table 3.1: Protocol adjustments made during model development.

Problems	Changes Made	Possible Implications
Unable to achieve a 50% increase in LVEDP across pacing animals (EF below 30%) over 24-48 hours.	Change from using LVEDP to CO as an indicator of decompensation due to acute HF.	CO is a better indicator of cardiac dysfunction and impairment than an indicator of volume overload in this model.
Rhabdomyolysis, due to complete ligation of femoral arteries in microembolization affected the cardio-renal study.	Change from treadmill to sling experiments.	Unable to use exercise strain to induce acute decompensation.
The transition from treadmill to sling data collection.	No change to experimental design following treadmill to sling switch.	Comparison of treadmill and sling rest data revealed no significant difference in hemodynamic measurements.
Higher mortality rate due to aggressive pacing.	Gradually increasing the duration of pacing to achieve acute HF.	Lower mortality rate and increased appetite benefit.
The number of microembolizations necessary to achieve chronic HF at or below 30% EF began to exceed more than 11 (max) procedures affecting budget, time, instrument efficiency, and mortality.	Target EF of at or below 30% was changed to 40% EF or below. In addition, sonication was recommended for use during procedures.	Shortened the time necessary to achieve chronic HF by half and adequate decompensation was present despite the higher EF endpoint.
Instrument failure became a problem after 6 months' time. Catheter tubing became brittle and was prone to cracking and clotting.	Took advantage of anesthesia dependent procedures and surgically implanted catheters at later time periods in the study protocol.	Increased the longevity of catheters.
Ventricular tachycardia and premature ventricular contraction episodes post-24 hours after CAM.	Administered propranolol pill orally, every 6 hours for 24 hours.	Minimized the incidence of fatal arrhythmias or other cardiac events that lead to mortality.
Anesthesia related effects on hemodynamics following inulin clearances.	Catheterization process was completed under 20 minutes maximum.	Reduced anesthesia effects on hemodynamics.
Dehydration of animals that may not have had fluids before inulin clearance.	Intravenous fluids were given for at least 30 minutes prior to inulin clearance.	Prevented dehydration related volume issues that may affect renal clearance collections.
Bulky osmotic infusion pump required constant 48-hour supervision of the animal and administration line within a metabolic cage.	Switched to a mini infusion pump which could be packaged inside the canine's t-shirt and jacket. Checked the infusion pump every 4 to 8 hours.	Ensured proper drug delivery with the animal in its normal housing facility. This decreased anxiety for the animal and prevented the handler from monitoring the metabolic cage continually.
One lab oversaw both data collection, drug delivery, and data analysis.	Standardized certain tasks to separate labs and personnel. A third party prepared the serelaxin and placebo infusion.	Ensured a properly randomized double-blind study.

This table includes problems, changes made, and possible implications to study design that occurred during model development. See text for the definition of abbreviations.

By consensus, we empirically elected to shift our target to a 20% reduction in CO from the averaged CO measured post-HF experiments. A reduction in CO was considered to be a robust physiological indicator of acute cardiac dysfunction and proved consistently achievable with our experimental methods.

Experimental protocol

Our model is intended to serve as an accurate, experimental environment to test new drugs for the management of acute HF. To ensure that we achieve a state of acute decompensation that is translationally relevant, we targeted a sustained CO reduction of at least 20% for three hours after discontinuation of pacing. To measure this, animals were brought to the lab the morning after initiation of pacing, and hemodynamic rest data were collected for at least 15 minutes. Pacing was then discontinued, and the animal was monitored for another three hours. At three hours, CO was re-measured for 15 minutes. The calculated average CO was obtained and compared to the mean CO post-induction of ICM. If a sustained reduction in CO was not achieved, pacing was resumed for another 24-48 hours, and CO was reassessed in the same manner. This cycle was repeated until a persistent CO reduction was seen. The animal was then considered to have achieved the status of ‘acute HF’ and would be ready for enrollment into a drug trial, with subsequent measurement and analysis of hemodynamics, LV function, inulin clearance, and other study endpoints of interest for days-weeks following randomization.

Following the completion of the experimental protocol, the canines were euthanized according to American Veterinary Medical Association (AVMA) guidelines with pentobarbital (100 mg/kg) IV.

Statistical analysis:

Plasma concentrations of NT-proBNP were quantified using a commercially

available canine-specific ELISA kit (Kamiya Biochemical Company, Seattle WA, catalog # KT-23770) as per the manufacturer's instructions. A 96-well plate reader was used to measure the results. A 1-tailed ANOVA was utilized to statistically measure the lab values. Results and statistics for the canines in the protocol (n=10) were plotted using Prism 9.1.0 (version 216, Graphpad, LLC).

RESULTS

Our initial experience shows that our novel CAM/RVP model provides a reliable method of inducing acute decompensation of chronic HF (due to underlying ICM). Given the success of our approach, we propose this to be a generalizable approach to test novel HF therapeutics aimed at acute HF. As shown in Figure 3.3 a significant reduction in EF

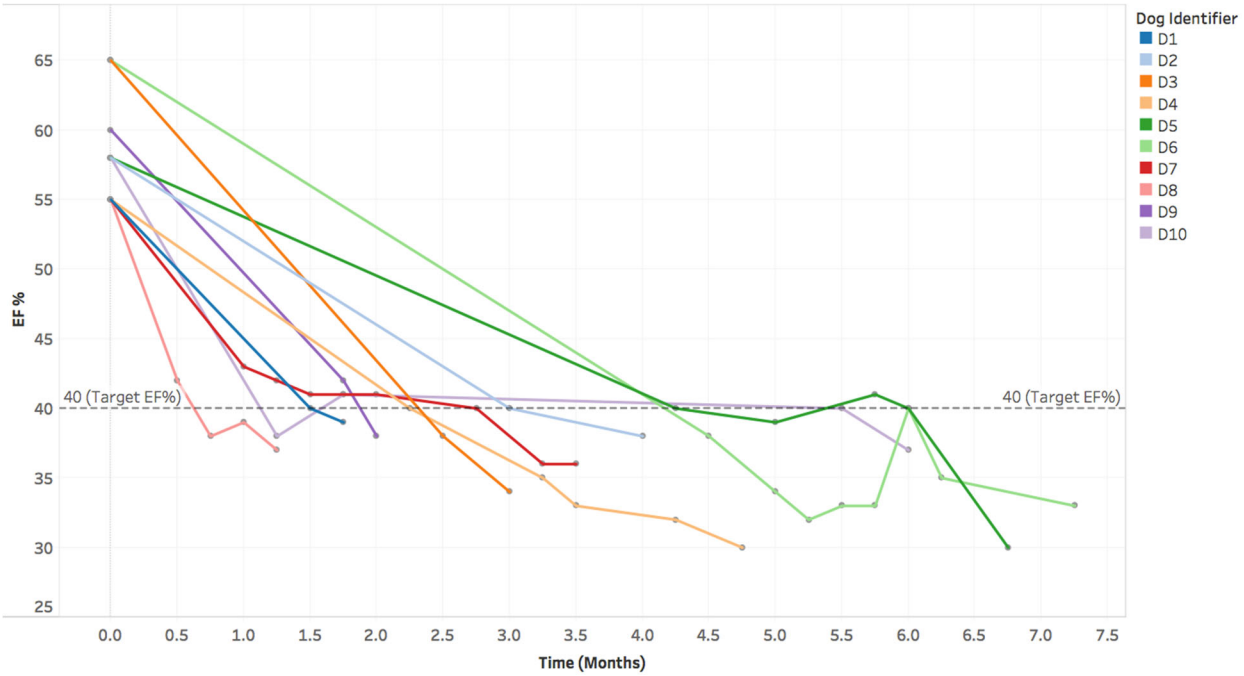

Figure 3.3: Ejection fraction over time. Qualitative measurements of EF taken during the CAM procedure for canines (n=10) over an approximately 7.5-month period. Target EF was 40% as identified by the horizontal dashed line. See text for definition of abbreviations.

was achieved with CAM, and the goal of 30-40% proved to be attainable. Moreover, the CAM procedures modeled ICM without an acute perturbation, as shown by assessment

of NT-proBNP. Mean values of NT-proBNP (Figure 3.4) averaged approximately 300 pg/mL at baseline, remained stable at 300 pg/mL following confirmation of ICM, and increased significantly (p=0.0371) to 600-800 pg/mL following pacing indicating myocardial stress and acute decompensation. Raw data for NT-proBNP protein concentration for the canines (n=10) are available in the online supplement. This significant (p=0.0057) increase was maintained for our observation period of 30 days and indicates that the animals were in a state of stable compensation prior to RVP.

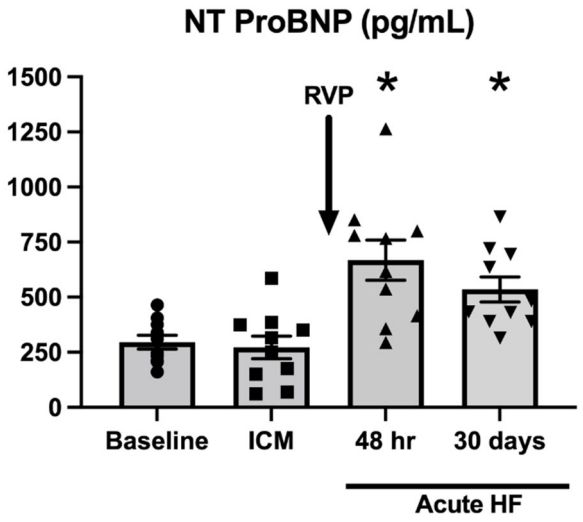

Figure 3.4: NT-proBNP values during acute-on-chronic HF protocol. Average NT-proBNP (pg/ml) concentrations in canines (n=10) with accompanying standard error bars are shown. Onset of RVP and the acute HF state is denoted by vertical and horizontal black bars respectively. Individual measurements are reported during baseline (black circle), ICM (black square), 48-hours post-RVP (black triangle pointing upwards), and 30 days post-RVP (black triangle pointing downwards). See text for definition of abbreviations. Statistical significance between subsequent timepoints is shown as * $p \leq 0.05$ versus ICM.

DISCUSSION

It has previously been shown that while there are may not be overt signs of cardiac dysfunction after embolization recovery, the contractile myocardium is damaged morphologically [151]. In moderate CAM preparations, myocardial remodeling can recover diastolic and systolic contractility even with permanent LV dilation[121]. This is reflected in the marked variability in time and number of repeat embolizations necessary to produce ICM (Figure 3.3): a total of 5-20 microembolizations were required, with 2 weeks-6 months needed to achieve the target EF $\leq$ 40%. Raw data for ejection fraction for the

canines (n=10) are available in the online supplement. Accordingly, this inherent variability in the model that may be a reflection of what occurs in humans clinically, must be accounted for in study design.

More aggressive CAM endpoints with EF's < 30% can cause NT-proBNP elevation representative of more severe HF [152] and should be considered in the future, though caution is needed to avoid fatal infarctions. The acute HF endpoint set as a CO reduction of 20% also proved to be attainable. As an acute precipitant, RVP mirrors the clinical situation in which patients with extensive coronary artery disease suddenly experience atrial or ventricular tachycardia, exacerbating underlying ICM and overcoming established compensatory mechanisms by increasing myocardial strain [151]. As shown in Figure 3.4, elevated NT-proBNP levels seen from following pacing and induction of acute HF confirm that, indeed, a sufficient degree of myocardial stress resulted from the pacing procedure coupled with the already damaged myocardium. Importantly, the level of acute cardiac stress induced was sufficient to trigger a moderate degree of physiological decompensation while avoiding negative outcomes.

Overall, the utility of this model is strengthened by the ability to assess the degree of HF in the conscious state, eliminating potential concerns about whether cardiac and renal hemodynamic findings are altered by sedation. It also has the advantage of enabling serial monitoring to observe how interventions affect both the pathophysiologic state.

The causes of HF are diverse, often multifaceted, and difficult to incorporate into large animal models [72,111]. As discussed previously, simple models of HF are not enough to successfully transition from basic science research to clinical intervention [71,72,111]. We hope our experience can serve as a template and thus accelerate the creation of other novel acute HF models using different combinations of acute and chronic dysfunction in

order to investigate specific phenotypes of interest. For example, hypertension, myocardial infarction, and aortic banding devices could be used to produce underlying ICM. Likewise, methods to induce acute decompensation may include pre-load and afterload stressors, myocardial ischemia, and RVP. Each alteration in the model could be thoroughly evaluated using the methods we have outlined, and importantly, complications can be closely monitored. New combinations and alterations of precipitants and underlying substrate can be predictably burdened by unforeseen complications; thus, careful research and inquiry are required before execution.

In conclusion, high clinical translation of large animal models for novel drug testing in acute HF depends on the model's ability to closely reproduce the complex causes of this condition in humans. The combination of ICM with an isolated episode of tachycardia induced decompensation is a novel approach to the study of acute HF, improving upon existing models. Our CAM/RVP protocol represents an advance in the means to accurately assess new therapeutic interventions in the setting of acute HF and serves as a guide for future research and development of multifaceted acute HF models. While model creation is a labor-intensive process that requires a great deal of patience and recognition of unanticipated complications, the development of an appropriate response helps to ensure scientific rigor and reproducibility. Therefore, this newly synthesized canine model of acute HF will be effective in evaluating the hypotheses identified in Chapter 2.

CHAPTER 4 – DECIPHERING THE EFFECTS OF SERELAXIN ON THE CARDIORENAL AXIS IN ACUTE HEART FAILURE WITH UNDERLYING ISCHEMIC CARDIOMYOPATHY

ABSTRACT

Objectives: To evaluate the cardiorenal effects of SLX using a novel canine model of acute HF. Background: SLX showed promising preliminary data in humans with acute HF but failed to provide outcomes benefit when tested in an adequately powered clinical trial, and intermediate mechanisms of possible benefit remain unestablished. Methods: Chronic ischemic cardiomyopathy was initiated in 10 canines via repeated coronary microembolizations until an ejection fraction ≤ 40% was achieved. Acute HF was then induced via overdrive pacing targeting a 20% reduction in cardiac output. Upon achievement of acute HF, a 48-hour infusion of serelaxin or placebo was delivered. Hemodynamic, renal function, and biomarkers were compared between induction of acute HF (0 hr) and post-treatment during several timepoints over 30 days. Animals were then sacrificed, and post-mortem histological comparisons were performed. Results: No significant differences were observed in cardiac and renal hemodynamics between placebo (n=5) and serelaxin (n=5) following acute HF induction. NT-proBNP and troponin concentrations increased in both groups with the onset of acute HF, but there was no difference in attenuation over 30 days between treatment groups. There were also no histological differences on renal and myocardial tissue post-mortem analysis. Conclusion: Using a canine animal model of acute HF, a 48-hour infusion of SLX produced minimal hemodynamic, biomarker, or histological effects. These data are congruent with the absence of benefit in the pivotal clinical trial and suggest that future drug development programs in acute HF may benefit from the early establishment of proximate mechanism of action via animal models.

INTRODUCTION

Acute HF is a common, high burden condition that typically presents as a rapid worsening of symptoms in patients with ischemic cardiomyopathy and is often precipitated by abrupt changes in salt load, blood pressure or heart rate [99,153]. The pathophysiology of acute HF is complex involving systolic and/or diastolic LV but also an interplay of dysfunction between the heart, lungs, peripheral vasculature, and kidneys [6,153] as well as inflammatory responses, fibrosis, and overall worsening of cardiorenal hemodynamics [40,84,154-158]. Despite interest and resources towards novel therapeutics to treat acute HF, pivotal trials have largely failed, including drugs with promising preliminary data [7,15,22,27,55,58,77,108]. A better understanding of why drugs succeed or not in pivotal trials is essential for future developmental efforts to improve the efficiency and pace of development [8,21,41]. This study seeks to elucidate the effects of SLX on cardiac and renal hemodynamics and test the hypothesis listed in Chapter 2.

METHODS

A general overview of our study protocol and corresponding time frames for specific procedures and measurements is shown in Figure 4.1, with angiographic evidence of instrumentation shown in 4.2. Study procedures were employed using the methodology previously reported in Chapter 3, inulin clearance experiments will be referred to as renal function test (RFT) for this chapter.

Experimental subjects/animal handling

Ten mongrel dogs (6 females, 4 males; 21-27 kg) were chronically instrumented for hemodynamic measurements. All animals were acclimatized to the laboratory surroundings. All the procedures were approved by the IACUC of Wayne State University and complied with the National Institutes of Health *Guide to the Care and Use of*

Laboratory Animals. Before study procedures commenced, all investigative staff members were blinded to the drug, and the canines were randomized into either placebo or SLX treatment groups.

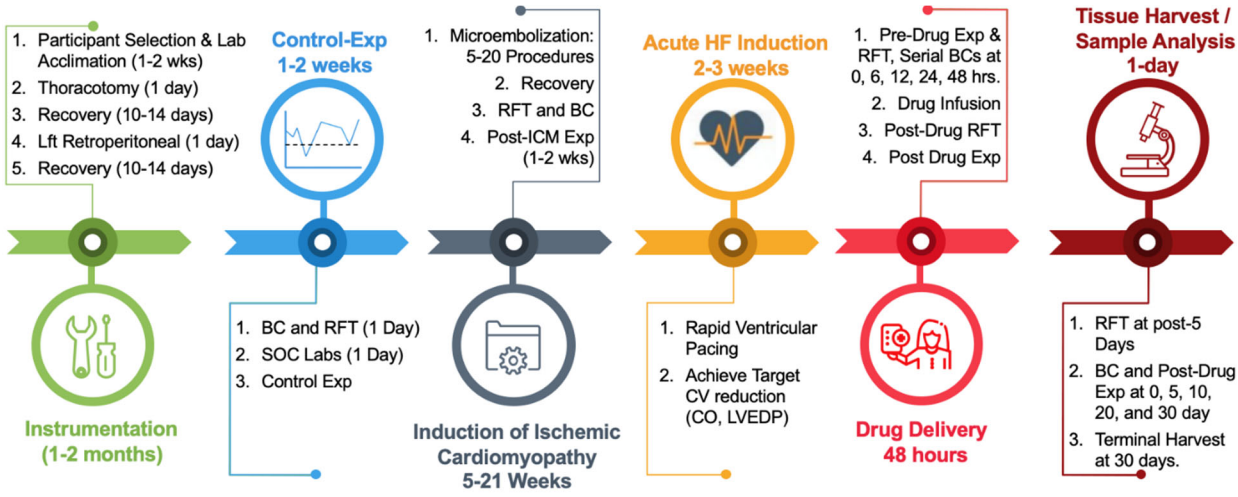

Figure 4.1: Timeline of experimental procedures. Outline of canine SLX-study procedures with time.

Serelaxin/placebo infusion

Achievement of acute HF for this study was defined as a sustained reduction of CO ≤ 20% for 4 hours post-discontinuation of external pacing. Once this was demonstrated, the SLX/placebo infusion protocol was initiated. First, pre-treatment hemodynamic data along with blood for biomarker analysis and void urine for inulin clearance were collected. Second, IV saline and FITC inulin were infused for 1 hour to achieve a steady state, which was established as the acute HF/0 hr timepoint. Finally, drug infusion then commenced and based on the randomization scheme, either placebo or SLX (30 μg/kg/min) was administered for a period of 48 hours. All canines were placed in the sling only during data collection (30 min) at 0, 6, 24, 48 hours following initiation of the infusion. Inulin clearance was reassessed immediately upon completion of the 48-hour infusion, and at 5 days post-infusion. Blood samples for biomarker analysis and

hemodynamic data were collected at 0, 6, 24, and 48 hours during the infusion and at 5, 10, 20, 30 days post-infusion.

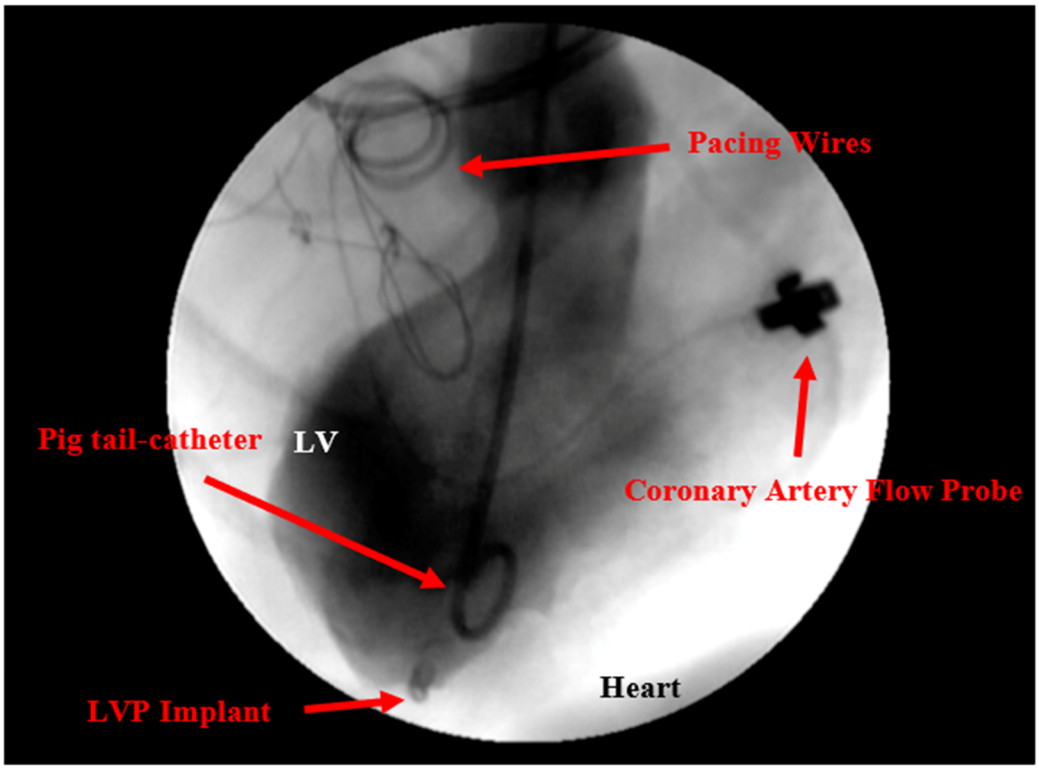

Figure 4.2: Angiogram of heart undergoing CAM to induce ICM. The angiograph is from a female mongrel-bred canine that shows the placement of pacing wires, cardiac output flow probe, coronary artery flow probe as well as the pig tail catheter inserted into the left ventricle to infuse the isovue contrast agent to qualitatively measure EF.

Data acquisition

All experiments were performed after the animals had fully recovered from surgery, with specific attention on thermoregulation, body condition scoring (BCS), and general activity. Based on qualitative serial observations utilizing BCS, the degree of HF in our model may best be categorized as the New York Heart Association (NYHA) functional class 2 [30]. Hemodynamic data were collected throughout the study using standard procedures, as shown in Figure 4.1. Procedures/experiments commenced between 07:00 and 08:00 hrs to account for any diurnal variations. Each animal was brought into the laboratory and allowed to roam freely and acclimate for 10-20 min before being placed in

a sling designed to restrain movement in the upright position while allowing full weight-bearing. The CO, CBF, and RBF flow probe cables were connected to flowmeters (TS420, Transonic Systems), and the telemetry-based LV transmitter was turned on to collect data (DSI). The arterial catheters were aspirated, flushed, and connected to pressure transducers (Transpac IV, ICU Medical). Animals were observed until resting hemodynamic data were noted to be stable (typically 5-10 min). All hemodynamic variables were then collected in real-time with waveforms acquisition using an analog to digital data system (Labscribe 3, iWorx, Dover, NH).

Biomarkers

NT-proBNP as well as troponin (both I and T components) was assessed via blood plasma/serum and cardiac tissue samples collected throughout the protocol as indicated in Figure 4.1.

Terminal harvest

As described in Chapter 3, after 30 days animals were euthanized to measure protein adaptations and fibrosis. The canines were euthanized according to AVMA guidelines with pentobarbital (100 mg/kg) IV. The heart and kidneys were removed intact using a non-sterile surgical procedure, and tissue samples were harvested on-site and prepped within minutes of collection. After proper fixation, samples were stored in a -80°C freezer and only thawed once before analysis.

Data analysis

All hemodynamic data, including MAP, CO, HR, RBF, and LVP were continuously recorded during each experimental procedure. Other hemodynamic parameters were calculated during off-line data analysis [e.g., total vascular conductance (TVC), renal vascular conductance (RVC), maximal rate of rise in LVP (dP/d*tmax*), maximal rate of fall

in LVP (dP/d*tmin*)]. TVC, RVC, and cardiac power (CP) were calculated as CO/MAP, RBF/MAP, ((MAP x CO)/451) [159,160] respectively. Arterial elastance (E_a) was measured as End Systolic Pressure/SV [80]. One-minute averages of all variables were taken during steady-state at rest to maintain consistency across all conditions. Hemodynamic data are reported as means ± SE. An α-level of $P < 0.05$ was used to determine statistical significance. Average responses for each animal were analyzed with Systat software (Systat 11.0). A two-way ANOVA with repeated measures was used to compare hemodynamic data for time effect and/or condition effect between treatment vs control. In the event of a significant treatment effect, sidaks post-hoc test was used. For RBF, a mixed model comparison rather than ANOVA was used to account for missing data values in the SLX cohort.

Inulin clearance rate was measured using standard methods of FITC inulin preparation and flame photometry/plate reader analysis [85,149,150,161]. Plasma and urine samples were assessed for sodium and potassium by flame photometer [150,162]. Measures of P_{Na}, $U_{Na}V$, U_KV, C_{in}, FE_{Na}, and FE_K were then calculated using standard equations and compared between treatment groups and within groups using K matrix and multivariate analysis [150]. Statistics were applied using SPSS software (Version 25.0, IBM Inc. Chicago, IL) using one or two-factor parametric ANOVAs to examine mean differences between factor groups and time points of measurement. A Sidak post-hoc test was utilized, and a homogeneity of variance was checked and verified.

Plasma concentrations of NT-proBNP were quantified using a commercially available canine-specific ELISA kit (Kamiya Biochemical Company, Seattle WA, catalog # KT-23770) as per the manufacturer's instructions. A 96-well plate reader was used to measure the results. A 2-factor ANOVA (for group and time) was utilized to statistically

measure the lab values.

Troponin I and T in cardiac tissue samples were assessed via SDS-polyacrylamide gel electrophoresis (SDS-PAGE) and Western blot analysis where frozen muscle was directly homogenized in SDS-gel sample buffer containing 2% SDS and heated at 80°C for 5 min to avoid protein degradation [163,164]. The SDS gels used were 14% acrylamide/bisacrylamide at the ratio of 180:1. Monoclonal antibodies against cardiac troponin I (cTnI) and cardiac troponin T (cTnT) were used for the Western blot [163,164]. SDS-glycerol gel electrophoresis was applied to assess the expression of cardiac myosin isoforms as described previously (63). Blood serum samples were quantified for cTnI and cTnT, using canine-specific ELISA kits (Biotang Inc, Lexington, MA, Item# CA0544) as per the manufacturer's instructions.

RESULTS

Ventricular function and arterial elastance

Figure 4.3 shows the measures of LV function in all animals (n=10) during distinct time periods within the study. Hemodynamics were measured in both SLX and placebo treated animals to examine the impact of treatment on acute HF induced by RVP at time 0 hr. MAP did not show significant change over time following 0 hr in SLX treated animals whereas in placebo treated animals MAP significantly improved from 0 hr (Figure 4.3A). Neither placebo nor SLX infusion showed a significant effect on heart rate, though in the SLX group there was a significant reduction in HR over time between day 10 to day 30 from 0 hr (Figure 4.3B). Contractility (dp/dt_{MAX}) and lusitropy (dp/dt_{MIN}) were not significantly impaired between either treatment group by CAM; however, both were significantly attenuated by RVP at time 0, in accordance with our acute HF model. Additionally, in both treatment groups, we observed that dp/dt_{MAX} and dp/dt_{MIN} improved

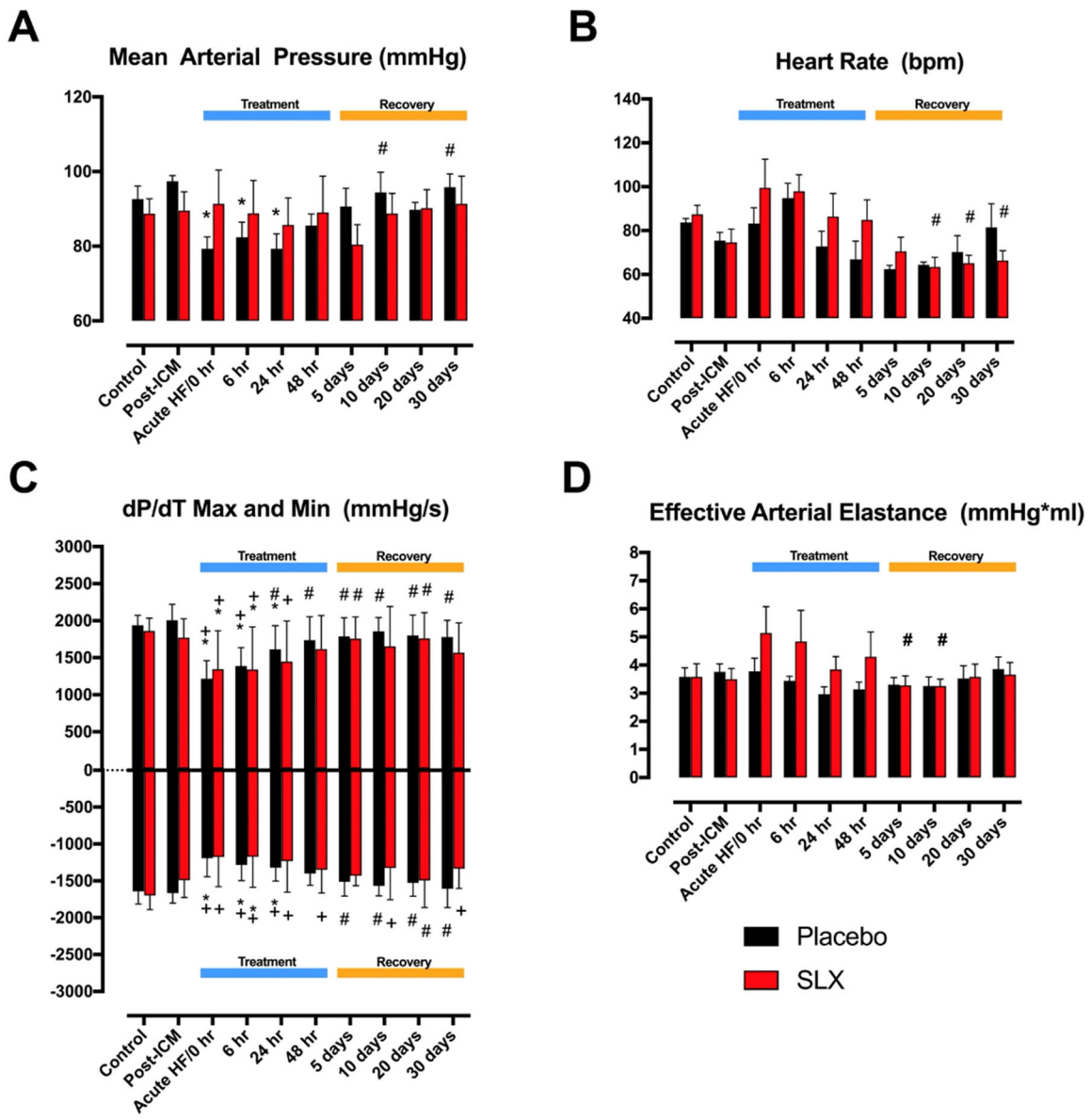

Figure 4.3: Ventricular function following serelaxin infusion. (A-D) Shows averaged 2-min steady-state values with accompanying standard error bars for mean arterial pressure, heart rate, dP/dT_{MAX} & dP/dt_{MIN}, and effective arterial elastance (E_a, end-systolic pressure divided by stroke volume). Each parameter was measured during baseline, chronic ischemic cardiomyopathy (post-ICM), the onset of acute HF and treatment (acute HF/ 0 hr), remainder of the 48hr treatment period (6, 24, 48 hr) denoted by the horizontal blue bar and during recovery (5, 10, 20, 30 days) denoted by the horizontal orange bar. Placebo (n=5) and SLX (n=5) cohorts were delineated by black and red bars, respectively. Statistical significance between subsequent time points are shown as * $p \leq 0.05$ versus post-ICM, # $p \leq 0.05$ versus 0 hr (acute HF), + $p \leq 0.05$ versus baseline.

post-infusion, beginning at 24 hr from the onset of infusion to day 30 (Figure 4.3C). E_a did

not increase significantly during or post-infusion in either treatment group (Figure 4.3D). However, in the SLX group there was a non-significant rise in E_a, indicating ventricular-vascular uncoupling at time 0 with statistically significant recovery following treatment at 5 and 10 days toward pre-acute HF levels. No interaction was found between treatment groups in any of the hemodynamic variables.

Cardiorenal axis

Figure 4.4 A-D shows the average values for CO, SV, RBF, and CP over time. For

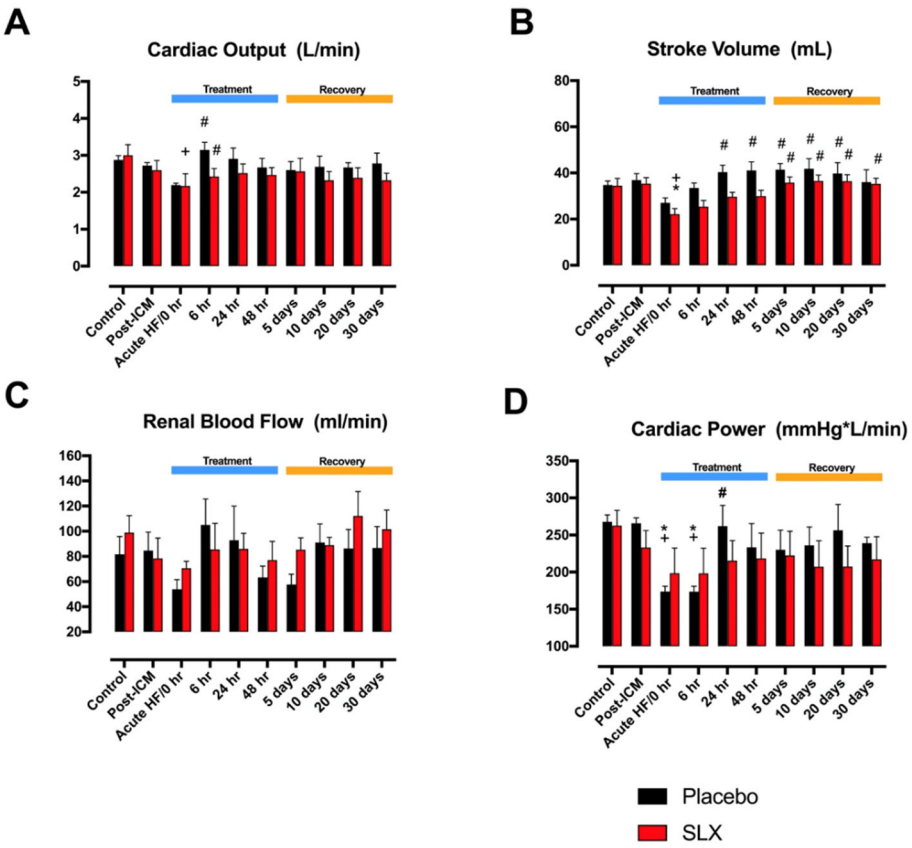

Figure 4.4: Overall cardiac function following serelaxin infusion. A-D Shows averaged 2-min steady-state values with accompanying error bars for cardiac output, stroke volume, renal blood flow, and cardiac power (calculated as CO × MAP). Each parameter was measured during baseline, chronic ischemic cardiomyopathy (post-ICM), the onset of acute HF and treatment (acute HF/ 0 hr), remainder of the 48hr treatment period (6, 24, 48 hr) denoted by the horizontal blue bar and during recovery (5, 10, 20, 30 days) denoted by the horizontal orange bar. Placebo (n=5) and SLX (n=5) cohorts were delineated by black and red bars respectively. Statistical significance between subsequent timepoints is shown as * $p \leq 0.05$ versus post-ICM, # $p \leq 0.05$ versus 0 hr (acute HF), + $p \leq 0.05$ versus baseline.

both treatment cohorts, CO increased at 6 hrs, but no further improvements were noted. SV increased (Figure 4.4B) at 6 hrs post-infusion and continued throughout the recovery period for placebo-treated animals. In contrast, no difference in SV was noted until day 5 in the SLX treated group, which was also sustained throughout the recovery period. Of note, SV was lower at the 0 hr compared to measurements pre-ADHF in the SLX group but not in the placebo group. RBF is shown in Figure 4.4C. Despite an apparent decrease in RBF at time 0, there was no significance across timepoints. CP (Figure 4.4D) was significantly lower compared to pre-ADHF levels at 0 and 6 hrs and increased compared to 0 hr at 24 hrs in the placebo group. No significant change in CP was observed over time in the SLX treated group. Following analysis of these measures, though there were significant changes within both groups, there was no effect of treatment between the cohorts.

Biomarker data

NT pro-BNP and troponin were selected as indicators of ADHF [164,166,167] to determine the degree of recovery following SLX infusion. NT-pro BNP data (Figure 4.5A) showed no significant effect over time, either between or within groups. Troponin I and T values increased post-infusion with a wide level of variability (Table 4.1 and Table 4.2). Western blots and SDS-glycerol-PAGE results (Figure 5B-E and Table 4.2) did not show any significant change in troponin I, troponin T, and myosin isoform expressions. In both treatment groups, there was no discernable degradation of cTnI and cTnT. Western blot data in Figures 4.5B and 4.5C further showed similar data between treatment groups, which correlated with the values for serum troponin in the samples (n=10).

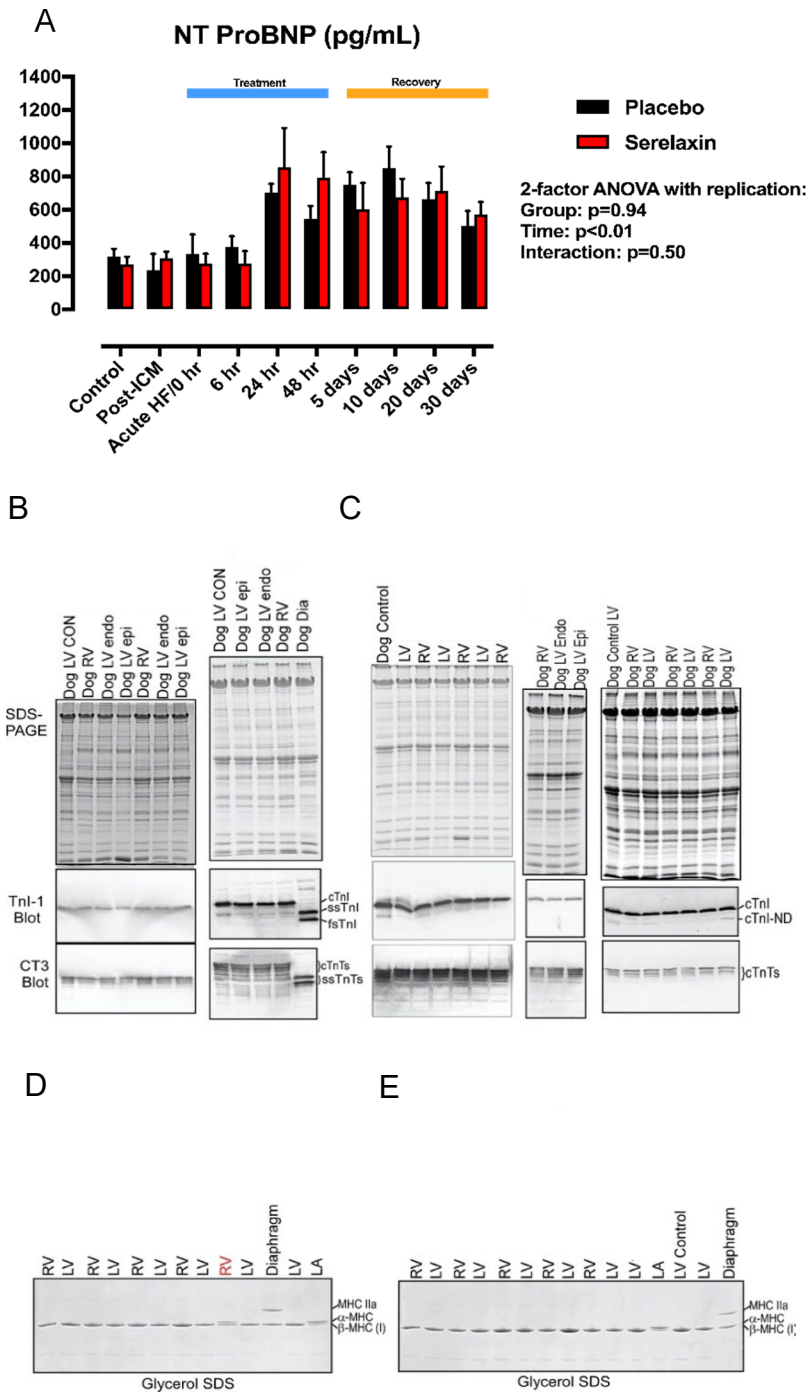

Figure 4.5: Biomarker results in both placebo and serelaxin cohorts. Troponin Analysis of the SDS Page NT-proBNP results. A: NT-proBNP levels from baseline to post 30 days infusion (n=10). B-E: SDS page results from the left and right ventricular epicardium and endocardium, and MHC adaptor proteins, including control gels.

Figure 4.5D and 4.5E showed similar results for expression of myosin heavy chain (MHC) α/β, indicating insignificant chronic adaptation in the RV and LV endocardium.

Table 4.1 did not show increases except in cTnI-ND and MHC α when collected during the terminal harvest post day 30. Serum cTnT results are shown in the Supplement Table 3.

Table 4.1: Summary of TnI protein concentration following SLX treatment

TnI (pg/ml)	SLX Treated (n=5)					Placebo Treated (n=5)				
Control	29	29	40	ND	ND	ND	ND	46	36	ND
Post-ICM	39	ND	27	32	40	44	35	31	28	ND
Acute HF/0 hr	31	28	42	32	53	42	33	33	33	33
6 hr	33	36	29	ND	ND	ND	ND	30	28	ND
24 hr	33	30	28	47	32	34	56	48	41	0
48 hr	32	40	30	35	31	31	31	49	39	45
5 days	37	28	42	ND	ND	ND	ND	33	49	50
10 days	33	30	33	34	36	27	33	33	34	55
20 days	30	31	30	42	37	34	33	29	39	27
30 days	34	ND	29	ND	ND	ND	ND	31	32	ND

TnI concentration following analysis of blood serum samples between placebo and SLX treated canines. ND denotes not determined. Each column represents an individual animal.

Table 4.2: Summary of Myofilament Protein Adaptation

	LV Endocardium				RV			
	cTnT-ND	**cTnI-ND**	**α-MHC**	**β-MHC**	**cTnT-ND**	**cTnI-ND**	**α-MHC**	**β-MHC**
Placebo	-	-	-	+	-	-	-	+
Placebo	-	-	-	+	-	-	-	+
Placebo	-	-	-	+	-	-	-	+
Placebo	-	-	-	+	-	-	-	+
Placebo	-	Increase	-	+	-	-	-	+
SLX	-	-	-	+	-	-	Increase	Decrease
SLX	-	-	-	+	-	-	-	+
SLX	-	-	-	+	-	-	-	+
SLX	-	-	-	+	-	-	-	+
SLX	-	-	-	+	-	-	-	+

Quantification of myofilament proteins in the LV endocardium and the right ventricle following end of study terminal tissue harvest (n=10). NH_2-terminal truncated cardiac troponin T and I (cTnT-ND or cTnI-ND) and both alpha and beta isoforms of myosin heavy chain (α-MHC and β-MHC) are presented. The presence or absence of detected proteins is denoted by + or – respectively, and increases or decreases are labeled as such.

Renal function using inulin clearance

Little to no significance was found across each timepoint or between treatment cohorts with respect to inulin clearance, RBF, HR, Plasma Na and K, urine volume, $U_{Na}V$,

U_KV, FE_K, FE_{Na}, and MAP during the measurement period (see supplement Tables 4.1 and 4.2 for measures of median/IQR and mean/SD respectively).

DISCUSSION

This is the first study to test the efficacy of SLX in treating acute HF using a highly translatable conscious canine model. We found that SLX overall does not have a significant impact on the cardiorenal axis, making it unlikely to have a significant clinical effect in the setting of acute HF.

SLX impact on ventricular function, vascular response, and the cardiorenal axis

SLX's reported effects on the cardiovascular system during acute HF have included vasodilation and the reduction of aberrant remodeling that follows cardiac injury [9,10,21,50,84,86,96,167]. As such, we anticipated that increased LV function, improved arterial elastance, and a shift in cardiorenal hemodynamics towards pre-acute HF levels with SLX treatment. Yet, positive recovery following SLX was not consistently demonstrated. In fact, when looking at SV, there was a seemingly better return of function observed in the placebo than the SLX group suggesting that SLX had a limited if not detrimental effect on stroke work [168]. Assessment of MAP did not show a significant impact of HF nor treatment, which may be attributed to the length of time of the study or other compensatory mechanisms like remodeling and/or increased blood flow to collateral vasculature in canines [169].

E_a was calculated in effort to gain insight into the ventricular-vascular coupling relationship or, more specifically, an index of cardiac cycle time decay, resistance, and pressure. It has been shown in canines that baseline E_a values are between 3.0-4.0 (with human values between 0.6-1.2), which was also observed in this study [160]. Across both treatment groups during the CAM-induced reduction in LVEF and subsequent induction

of acute HF, a rise in E_a was observed, indicating disruption in the flow-pressure dynamic from baseline values. While there was a greater rise in E_a for the SLX group, it was not statistically significant and no longer present at 5 days post-treatment. Further, no other relationship was found to indicate that SLX increased RBF, glomerular filtration rate, or renal excretory function. Ultimately, as in the case with all of the hemodynamic measures collected in the study, no interaction existed between the placebo and SLX groups to suggest sustained treatment benefit to cardiac or renal structure and function.

SLX impact on renal function

Various studies have highlighted SLX's impact on the vasculature as vasodilator, which has prompted interest its ability to treat impaired renal function inherent in acute HF [10,86]. This study employed an RFT utilizing FITC-inulin over creatinine to confer a better measure of renal function during ICM and ADHF induction as well as after treatment. It was hypothesized that GFR (C_{in}) would improve following treatment, however, the results were inconclusive. RFT specific hemodynamics were collected during the procedures in effort to calculate functional measurements. As shown in supplemental tables 1-2, we did not observe any significant improvement in Na/K handling in plasma or urine samples nor in calculating fractional excretion of Na/K following SLX treatment. During the beginning of the study, treadmill exercise was being assessed. However, due to the CAM procedures ligating the femoral artery, we observed that one animal during the RFT procedure was positive rhabdomyolysis. This animal was removed from the study protocol for 30-day's time before reintroduced, and the RFT was performed again. Nevertheless, we did not observe significant variation to our measurements for that animal for the remainder of the study, even during the end-of-study comparisons with other animals. These results show that SLX does not impact renal

function.

Biomarker and tissue analysis

Tissue bloc analysis and troponin biomarker analysis displayed no significant improvement towards pre-acute HF. The anticipated decrease in troponin following treatment with SLX did not occur. Protein expression too did not indicate appreciable change between SLX and placebo groups. Additionally, the adaptor proteins did not increase or decrease in MHC IIa and MHC α/β [40,158]. Further, NT-proBNP results, too, did not show beneficial impact of treatment on heart failure. It has been previously reported that post-ICM at NT-proBNP levels were 2000 pg/ml, which is higher than the reported values in this study (between 600-900 pg/ml) [170]. The lower values reported could be the result of the degree of HF as well as the age and breed of the canines. Additionally, differences in sequence homology may be another culprit, for instance, if studies used a human-specific antibody, it may not reliably detect the presence of canine proteins. Finally, modified forms and fragments of NT-proBNP result in variations in molecular weight which impact measurements [171].

Myocardial tissue immunohistochemistry images reported in Figure 4.6, does illustrate interesting morphological impacts of our acute HF model as seen in Figure 4.6A where focal lesions developed following the embolization's which is in contrast to the dispersed collagen deposits that persist following RVP. It is very likely that a combination of focal and dispersed collagen deposition was present in the cardiac tissue by the end of the study. To that end, the method by remodeling was likely the result of microspheres targeting the left side of the heart (LAD and CX) coupled with RVP impacting the left ventricular free wall, which perhaps synergistically furthered the development of collagen and fibrosis in the cardiac tissue. Despite, structural and functional detriment of this

model, the analysis of the study results does not suggest any noticeable sustained impact results from SLX infusion. These data parallel the subsequent studies of the pre-RELAX trial that also reported little to no significance for SLX infusion in treating acute HF.

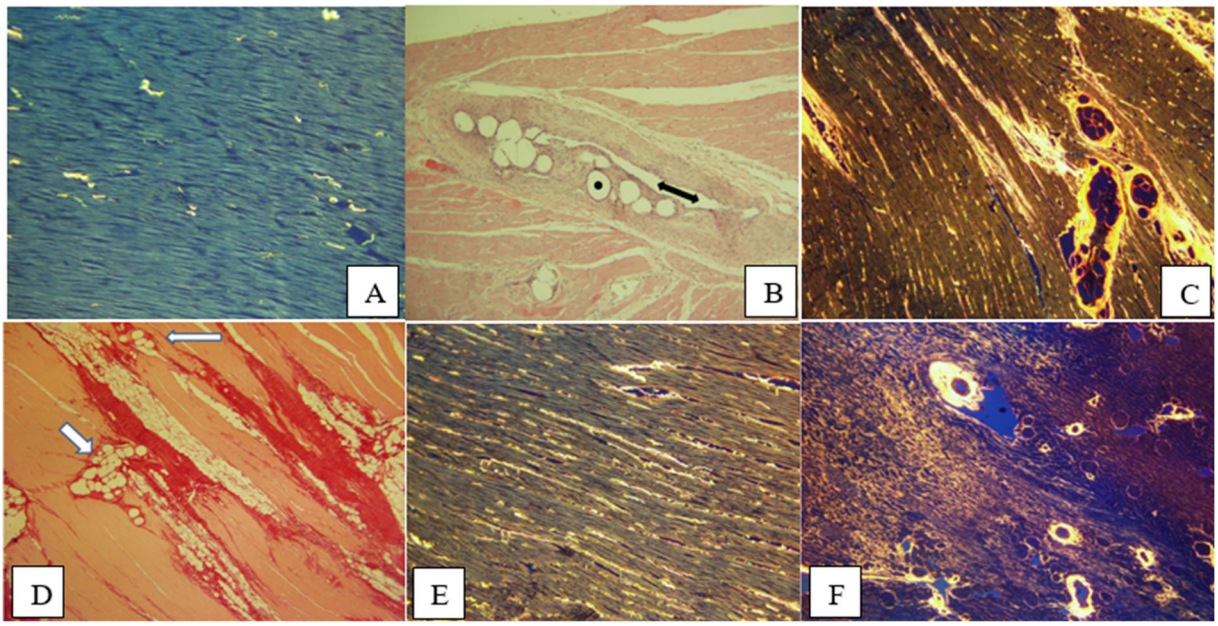

Figure 4.6: Immunohistochemistry of CAM vs RVP cardiac tissue and renal tissue. Using IHC, the image is stained with picrosirius red (PSR) and viewed with bright-field (BF) illumination. Panel 4.6a illustrates myocardial tissue derived from normal heart. Myocardium following microembolization-induced HF. Arrows show the focal lesions. Panel 4.6b, shows section stained with hematoxylin and eosin with BF illumination. The image depicts the architecture of intramyocardial arteries and collagen fibers. Likely showing impaired relaxation and increased arterial stiffness due to the structural change due to the microspheres. Panel 4.6c shows the focal nature of the lesions and the clumping of the latex microspheres. Panel 4.6d shows myocardial tissue following microembolization-induced HF whereas Panel 4.6e shows myocardium post-overdrive pacing (without microembolizations) with dispersed fibrosis and collagen deposition. Panel 4.6f shows focal lesions in renal samples following microembolizations.

Conclusion

In conclusion, these data provide a better understanding of the cardiac and renal hemodynamic mechanisms that are impacted following 48 hr infusion of SLX in the setting of acute HF. Using a highly translatable animal model, we found no cardiovascular or renal benefits with SLX treatment in the setting of acute HF. [165] These data also portend that our hypotheses were not correct in that 1) SLX did not positively improve the loss in

function in cardiac hemodynamics as seen after acute HF induction 2) SLX did not improve renal hemodynamics or function following induction of acute HF.

CHAPTER 5 – CONCLUSIONS

Overall, in accordance with our results, the significant findings in these studies were:

i) Our lab established a novel and highly translatable large animal model of heart failure with acute decompensation that enabled the recapitulation of human pathophysiology to test the effect of a 48-hr infusion of serelaxin.

ii) SLX treatment for acute-on-chronic HF did not recover 20% of the loss of function in cardiac hemodynamics and does not result hemodynamic or biomarkers improvement.

iii) Acute HF-induced renal impairment, though attenuated due to RVP, did not significantly improve over 30 days post-treatment with SLX.

To our knowledge, this is the first study to utilize two HF methods (CAM and RVP) in a highly translatable large animal species to create a novel model for treating acute HF while assessing implications to the heart and kidney. Utilizing histology and biomarker analysis, we noted significant injury to the myocardial wall due to focal and dispersed lesions caused by CAM and RVP, thereby validating that our model was indeed one of acute HF where an acute insult is superimposed on underlying chronic ischemic myocardial injury. [151,174,175].This study confers valuable insight into understanding of SLX in the treatment of acute HF to first responders and emergency room physicians alike particularly in the domain of medical knowledge. Understanding impact of SLX on physiological responses of acute HF benefits decision making and future analysis of study decision and execution for the evaluation of new treatment methods for scientists and clinicians.

Limitations

The primary limitations of our study design are based on the use of an artificially induced model of ischemic heart disease, which, depending on the individual animal, may impact the desired degree of cardiac dysfunction; with increased cardiac insults that could contribute potentially to premature death, while too little would result in an incomplete capture of the pathological state. For these reasons, acute HF is problematic to model due to its diverse etiology, where many concerns could impact treatment outcomes [153]. Accordingly, the use of mix-breed mongrel canines in this study does certainly engender variability into the data however it helps to mimic the implications of genetic variability observed and accounted for in larger-population phase III trials. Further, because we utilized chronic instrumentation in a conscious animal, there is potential for device failure, a circumstance that cannot be fixed midstream, thus precluding derivation of meaningful data from that device. However, chronic instrumentation provides the significant advantage of allowing measurements to be obtained in the conscious state unperturbed by the effects of acute surgery and anesthesia. Measures of blood collection used to identify NT-proBNP and troponin may have been impacted by improper freezing, collection methods, or by general user error. Though this study during its inception was sufficiently powered, it was skewed to the cardiac hemodynamic measurements and not the renal function procedures. Accordingly, the reduced sample size, due to early mortality, may have also been an impact factor in reaching significance. Finally, a significant concern in this study was the inability to exercise the animals due to the possibility of rhabdomyolysis [172] and/or premature mortality thus all measurements were in resting/sedentary-like conditions in a supported sling [100]. Therefore, conditions were not present to stress the diseased heart into a further decompensated state, a

phenomenon that occurs in older humans in heart failure and pathologies that result in sedentary-like state [41,173].

Future directions

SLX not having any significant impact in improving cardiac or renal parameters proved our null hypothesis correct. The findings mirrored what was observed in the human RELAX-AHF 2 trial however, if future consideration is made to some of the challenges within our model and with identifying the merits of recent studies, like Murphy et al., 2019, that have reported positive findings following titration of different study parameters perhaps future studies may report the positive impact of SLX infusion in recovering cardiac and renal structure and function associated with acute HF [176].

Within the context of this study, the neutral results reported in this translational study could have been a result of various factors deriving from limitations with either study design and/or SLX treatment. In terms of study design, in addition to the majority of complications reported in the aforementioned table 1.1, another component that may have confounded the results was tonic activation of the muscle metaboreflex (MMR). In our study procedures, we were unable to re-suture the femoral artery in any of our canines. As such, when the animal was standing for periods of up to 1 hour, it was likely possible that metabolite build-up may have occurred. For this reason, the “exercise challenge” in this study was removed, and the animals were kept in the sling for short periods of time. Nevertheless, increased hindlimb collateral circulation may have mitigated the activation of MMR. In summary, it stands to reason that hemodynamics may have been influenced by other mechanisms like MMR. In the future, we would try to suture the vessel rather than ligating the artery in effort to better minimize confounding factors to functional status assessment [177].

Our evaluation of the study objective also did not seek to compare calculated invasive calculated measures such as E_a to that of non-invasive measures of cardiac strain performed via echo imaging during the progress of HF. The latter may provide an alternative non-invasive measure of assessing the benefit of SLX in mitigating end organ damage and improving peripheral vasculature dysregulation [178].

Additionally, in Murphy et al.'s investigation of SLX, they hypothesized that the binding affinity of SLX with its receptor could be modified to increase the duration of time the ligand has with its substrate [176]. Further, they also identified that longer-term treat than that which was previously reported (either 48 or 72 hrs) should be extended to 28 days to mirror the length of time it takes to cause a reversal in remodeling. Though their observations and results were dependent on the severity of the underlying cardiomyopathy/remodeling, they reported positive conclusions that show that SLX is indeed effective in treating acute HF and fibrosis. For future explorative studies to assess SLX, especially using our ICM/RVP model of inducing acute HF, I would measure the degree modified SLX would have on hemodynamic mechanisms, especially during strenuous bouts of activity such as exercise. Further, I would also try to assess fibrosis and hemodynamic attenuation due to acute HF was abolished given the different length of time for treatment. Finally, assess mortality benefit over 30 days following treatment.

In conclusion, treatment options (and adjuvants) are imperative for patients with acute HF as time is a large factor. Reports from medical professions within the last year during pandemic have urged more emphasis be made on quick diagnosis and treatment of cardiac conditions to reduced negative outcomes [179]. Accordingly, our evaluation of SLX though non-significant, does not preclude SLX from still possibly being an efficacious therapeutic for the treatment of acute HF.

SUPPLEMENT

Supplemental Table 1: RFT: Assessment of renal function using inulin clearance using median values.

Supplemental Table 1: Renal Function (median values)										
	$Control_{RFT}$ (n=5/treatment group)		Post-ICM_{RFT} (n=5/treatment group)		Pre-SLX_{RFT} (n=5/treatment group)		Post-SLX_{RFT} (n=5/treatment group)		5 Days $Recovery_{RFT}$ (n=5/treatment group)	
	Control	SLX	Control	SLX	Control	SLX	Control	SLX	Control	SLX
MAP_{RFT} (mmHg)	115.9 (20.5)	106.6 (27.7)	103.2 (72.4)	90.5 (14.4)	101.4 (120.1)	88.3 (26.8)	93.0 (19.9)	81.5 (18.1)	93.7 (13.3)	94.5 (5.7)
HR_{RFT} (bpm)	95.8 (22.0)	97.6 (62.9)	95.0 (61.4)	92.9 (18.3)	96.6 (66.7)	107.0 (23.5)	97.6 (25.3)	79.4 (20.7)	87.9 (38.8)	104 (14.0)
CO_{RFT} (L/min)	3.4 (0.9)	4.1 (3.7)	3.9 (1.3)	3 (1.3)	3.4 (0.9)	3.1 (1.1)	3 (1.8)	3.7 (1.2)	3.3 (1.7)	4.3 (1.3)
RBF_{RFT} (mL/min)	83.7 (50.9)	82.3 (104.5)	64.2 (84.7)	70.4 (164.0)	64.2 (87.9)	55.9 (101.5)	66.5 (47.4)	67.6 (121.2)	90.1 (46.1)	104 (128.4)
Cin (mL/min/kg)*BW	13.5 (33.9)	47.1 (36.3)	14.2 (36.8)	22.8 (38.8)	15.4 (39)	31.5 (47.3)	49.4 (14.6)	26.8 (34.7)*	56.2 (7.9)	29.7 (35.5)
Avg P_{Na} (mM)	139.5 (16.3)	138.1 (16.6)	137.4 (14.6)	142.4 (16.1)	140.5 (11.0)	139.3 (15)	138.7(15.7)	143.3 (11.7)	139.2 (8.4)	141.7 (10.5)
Avg P_K (mM)	3.9 (0.9)	3.3 (0.6)	3.7 (1.0)	4.2 (0.8)	3.7 (0.6)	3.8 (5.7)	3.7 (0.9)	3.6 (0.8)	3.80 (0.9)	3.9 (0.7)
$U_{Na}V$ (µL/min)	21.6 (49.6)	4.5 (12.3)	55.3 (59.5)	3.0 (26.5)	20.3 (62.1)	4.7 (23.2)	25.5 (73.5)	16.8 (32.7)	52.5 (87.4)	6.3 (44.3)
U_KV (µL/min)	22.7 (13.7)	56.9 (59.4)*	23.6 (8.2)	34.2 (31.8)	25 (18.9)	30.2 (40.5)	11 (16.7)	29.1 (25)	31.3 (24.7)	30.7 (26.7)
FE_{Na}	39 (95.7)	26.5 (29.3)	55.3 (78.3)	23.7 (14.2)	41.9 (86.0)	35.3 (41.8)	29.1 (19.3)	27.4 (53.2)	31 (24.2)	13.1 (9.1)
FE_K	0.5 (1.8)	0.1 (0.1)*	0.7 (1.8)	0.1 (0.3)*	0.5 (1.8)	0.1 (0.3)	0.3 (0.9)	0.4 (0.5)	0.7 (0.8)	0.3 (0.4)

Inulin clearance, plasma solute concentrations, urine excretion and fractional excretion rates were assessed with corresponding hemodynamic measures during the SLX (n=5) /placebo (n=5) drug protocol in canines. Timepoints included control, post-ICM, pre-drug, post-drug, and 5 days recovery. Values are median (Interquartile Range); $^{*}P<0.05$ vs treatment group; $^{\#}P<0.05$ vs previous condition and time. Non-parametric Mann-Whitney U test for median differences was used.

Supplemental Table 2: RFT: Assessment of renal function using inulin clearance using mean values.

Supplemental Table 2: Renal Function (mean values)										
	$Control_{RFT}$ (n=5/treatment group)		Post-ICM_{RFT} (n=5/treatment group)		Pre-SLX_{RFT} (n=5/treatment group)		Post-SLX_{RFT} (n=5/treatment group)		5 Days $Recovery_{RFT}$ (n=5/treatment group)	
	Control	SLX	Control	SLX	Control	SLX	Control	SLX	Control	SLX
MAP_{RFT} (mmHg)	113.20 ± 11	103.7 ± 16.6	88.8 ± 50.8	95.03 ± 8.2	68.34 ± 62.9	91.25 ± 14.5	95.64 ± 10.7	85.27 ± 9.6	93.43 ± 6.7	101.50 ± 12.5
HR_{RFT} (bpm)	100.68 ± 13.0	99 ± 31.5	80.67 ± 46.2	88.8 ± 9.8	83.1 ± 48.6	103.8 ± 12.7	91.94 ± 13.2	85 ± 11.4	92.28 ± 20.65	103.8 ± 7.0
CO_{RFT} (L/min)	3.60 ± 0.4	4.50 ± 2.0	3.90 ± 0.8	3.07 ± 0.6	3.09 ± 0.5	2.95 ± 0.6	3.38 ± 1	3.45 ± 0.7	3.76 ± 1.0	3.99 ± 0.7
RBF_{RFT} (mL/min)	85.45 ± 27.5	117.52 ± 77.8	70.64 ± 48.1	98.95 ± 90	65.72 ± 48	65.45 ± 54.6	70.96 ± 25.6	101.13 ± 67.2	81.30 ± 25.9	104 ± 90.8
Cin (mL/min/kg)* BW	25.5 ± 19.6	51.4 ± 25.3	24.3 ± 20	30.8 ± 19.9	26.56 ± 20.6	38.98 ± 23	48.62 ± 7.6	24.64 ± 15.7	54.1 ± 5.9	28.22 ± 20
Avg P_{Na} (mM)	142.20 ± 9	136.22 ± 9.1	141.50 ± 9.7	144.82 ± 8.3	142.98 ± 7.6	140.68 ± 7.5	139.20 ± 8.6	138.28 ± 6.4	135.22 ± 9.8	142.82 ± 4.5
Avg P_K (mM)	3.89 ± 0.5	3.38 ± 0.3	3.76 ± 0.5	4.10 ± 0.4	3.88 ± 0.3	5.88 ± 4.9	3.74 ± 0.5	3.54 ± 0.4	3.70 ± 0.5	3.80 ± 0.3
$U_{Na}V$ (µL/min)	26.88 ± 21.5	7.68 ± 8.4	38.22 ± 31.3	11.64 ± 14.1	32.58 ± 32.1	13.84 ± 14.8	39.48 ± 39.6	13.34 ± 13.7	61.8 ± 32.8	19.36 ± 25.4$^{\#}$
U_KV (µL/min)	20.52 ± 7	63.01 ± 41.5*	44.2 ± 17.6	21 ± 5.8	41.8 ± 21.4	26.8 ± 10.3	33.6 ± 14.7	13.8 ± 10.1	35.2 ± 15.8	26.4 ± 13.2
FE_{Na}	55.44 ± 45.76	28.1 ± 18.5	54.52 ± 41.4	24.1 ± 8.7	55.78 ± 53.5	34.28 ± 20	25.12 ± 10.5	22.58 ± 21.4	36.76 ± 13.1	24.87 ± 14.5
FE_K	0.90 ± 0.9	0.11 ± 0.1	1.15 ± 1.1	0.18 ± 0.2$^{\#}$	1.04 ± 1.3	0.19 ± 0.2	0.55 ± 0.5	0.27 ± 0.2	0.88 ± 0.5	0.34 ± 0.3

Inulin clearance, plasma solute concentrations, urine excretion and fractional excretion rates were assessed with corresponding hemodynamic measures during the SLX (n=5) /placebo (n=5) drug protocol in canines. Timepoints included control, post-ICM, pre-drug, post-drug, and 5 days recovery. Values are mean ± SD; $^{*}P<0.05$ vs treatment group; $^{\#}P<0.05$ vs previous condition and time. ANOVA was used.

Supplemental Table 3: TnT (pg/ml) concentration from blood serum following SLX infusion.

TnT (pg/ml)	SLX					Placebo				
Control	0	16	17	ND	ND	23	18	ND	ND	ND
Post-ICM	0	ND	21	24	27	33	29	ND	20	22
Acute HF/0 hr	0	21	30	21	39	17	22	98	30	23
6 hr	0	21	18	ND	ND	16	22	ND	ND	ND
24 hr	0	0	28	21	26	0	27	86	22	21
48 hr	0	19	17	21	25	26	29	47	26	22
5 days	21	15	21	ND	ND	18	18	35	ND	ND
10 days	0	31	25	21	24	17	28	29	ND	27
20 days	27	52	26	21	25	17	21	ND	24	24
30 days	0	ND	20	ND	ND	17	23	ND	ND	ND

TnT (pg/ml) gathered during 10-stage steps of the protocol in both SLX and placebo cohorts are quantified via ELISA analysis. ND: Not determined.

APPENDIX A

IACUC PROTOCOL APPROVAL LETTER

WAYNE STATE UNIVERSITY

INSTITUTIONAL ANIMAL CARE AND USE COMMITTEE
87 E. Canfield, Second Floor
Detroit, MI 48201-2011
Telephone: (313) 577-1629
Fax Number: (313) 577-1941

ANIMAL WELFARE ASSURANCE # A3310-01

PROTOCOL # A 02-03-14

Protocol Effective Period: June 27, 2014 – February 28, 2017

TO: Dr. Philip Levy
SOM Emergency Medicine
6G4 University Health Center

FROM: Lisa Anne Polin, Ph.D.
Chairperson
Institutional Animal Care and Use Committee

SUBJECT: Approval of Protocol # A 02-03-14

"Deciphering the Cardiorenal Effects of Serelaxin in Acute Heart Failure"

DATE: June 27, 2014

Your animal research protocol has been reviewed by the Wayne State University Institutional Animal Care and Use Committee, and given final approval for the period effective **June 27, 2014** through **February 28, 2017**. The listed source of funding for the protocol is **Novartis Pharmaceuticals**. The species and number of animals approved for the duration of this protocol are listed below.

Species	Strain	Qty.	USDA Cat.
DOGS	Mongrels, either sex, over 1 year old and between 21—27kg	20	D

Be advised that this protocol must be reviewed by the IACUC on an annual basis to remain active. Any change in procedures, change in lab personnel, change in species, or additional numbers of animals requires prior approval by the IACUC. Any animal work on this research protocol beyond the expiration date will require the submission of a new IACUC protocol form and full committee review.

The Guide for the Care and Use of Laboratory Animals is the primary reference used for standards of animal care at Wayne State University. The University has submitted an appropriate assurance statement to the Office for Laboratory Animal Welfare (OLAW) of the National Institutes of Health. The animal care program at Wayne State University is accredited by the Association for Assessment and Accreditation of Laboratory Animal Care International (AAALAC).

REFERENCES

1 Van Camp, G. Cardiovascular disease prevention. *Acta Clin Belg* **69**, 407-411, doi:10.1179/2295333714y.0000000069 (2014).

2 Tanai, E. & Frantz, S. Pathophysiology of Heart Failure. *Compr Physiol* **6**, 187-214, doi:10.1002/cphy.c140055 (2015).

3 Virani, S. S. *et al.* Heart Disease and Stroke Statistics-2020 Update: A Report From the American Heart Association. *Circulation* **141**, e139-e596, doi:10.1161/cir.0000000000000757 (2020).

4 Virani Salim, S. *et al.* Heart Disease and Stroke Statistics—2021 Update. *Circulation* **143**, e254-e743, doi:10.1161/CIR.0000000000000950 (2021).

5 Ponikowski, P. *et al.* 2016 ESC Guidelines for the diagnosis and treatment of acute and chronic heart failure: The Task Force for the diagnosis and treatment of acute and chronic heart failure of the European Society of Cardiology (ESC). Developed with the special contribution of the Heart Failure Association (HFA) of the ESC. *Eur J Heart Fail* **18**, 891-975, doi:10.1002/ejhf.592 (2016).

6 Dunlay, S. M. & Roger, V. L. Understanding the epidemic of heart failure: past, present, and future. *Curr Heart Fail Rep* **11**, 404-415, doi:10.1007/s11897-014-0220-x (2014).

7 Machaj, F. New therapies for the treatment of heart failure: a summary of recent accomplishments. *Therapeutics and clinical risk management* **15**, 147-155, doi:10.2147/TCRM.S179302 (2019).

8 Levy, P. D. & Bellou, A. Acute Heart Failure Treatment. *Curr Emerg Hosp Med Rep* **1**, doi:10.1007/s40138-013-0012-8 (2013).

9 Díez, J. Serelaxin: a novel therapy for acute heart failure with a range of

hemodynamic and non-hemodynamic actions. *Am J Cardiovasc Drugs* **14**, 275-285, doi:10.1007/s40256-014-0069-0 (2014).

10 Murtaza, G., Siddiqui, A. & Hussain, I. Recent Progress in the Therapeutic Role of Serelaxin in Vascular Dysfunction. *Curr Protein Pept Sci* **19**, 1079-1087, doi:10.2174/1389203719666180709103020 (2018).

11 Myers, P. O., Bordessoule, A. & Tissot, C. Serelaxin for infant heart failure in congenital dilated cardiomyopathy. *Cardiol Young* **28**, 734-736, doi:10.1017/s1047951117002797 (2018).

12 Tietjens, J. & Teerlink, J. R. Serelaxin and acute heart failure. *Heart* **102**, 95, doi:10.1136/heartjnl-2014-306786 (2016).

13 Pang, P. S., Collins, S. P., Gheorghiade, M. & Butler, J. Acute Dyspnea and Decompensated Heart Failure. *Cardiol Clin* **36**, 63-72, doi:10.1016/j.ccl.2017.09.003 (2018).

14 Abdo, A. S. Hospital Management of Acute Decompensated Heart Failure. *Am J Med Sci* **353**, 265-274, doi:10.1016/j.amjms.2016.08.026 (2017).

15 Raj, L., Maidman, S. D. & Adhyaru, B. B. Inpatient management of acute decompensated heart failure. *Postgrad Med J* **96**, 33-42, doi:10.1136/postgradmedj-2019-136742 (2020).

16 Kurmani, S. & Squire, I. Acute Heart Failure: Definition, Classification and Epidemiology. *Curr Heart Fail Rep* **14**, 385-392, doi:10.1007/s11897-017-0351-y (2017).

17 Teerlink, J. R., Alburikan, K., Metra, M. & Rodgers, J. E. Acute decompensated heart failure update. *Curr Cardiol Rev* **11**, 53-62, doi:10.2174/1573403x09666131117174414 (2015).

18 Arrigo, M. *et al.* Precipitating factors and 90-day outcome of acute heart failure: a report from the intercontinental GREAT registry. *Eur J Heart Fail* **19**, 201-208, doi:10.1002/ejhf.682 (2017).

19 Rubio-Gracia, J. *et al.* Prevalence, predictors and clinical outcome of residual congestion in acute decompensated heart failure. *Int J Cardiol* **258**, 185-191, doi:10.1016/j.ijcard.2018.01.067 (2018).

20 Mentz, R. J. & O'Connor, C. M. Pathophysiology and clinical evaluation of acute heart failure. *Nature Reviews Cardiology* **13**, 28-35, doi:10.1038/nrcardio.2015.134 (2016).

21 Díez, J. & Ruilope, L. M. Serelaxin for the treatment of acute heart failure: a review with a focus on end-organ protection. *Eur Heart J Cardiovasc Pharmacother* **2**, 119-130, doi:10.1093/ehjcvp/pvv046 (2016).

22 Sinnenberg, L. & Givertz, M. M. Acute heart failure. *Trends Cardiovasc Med* **30**, 104-112, doi:10.1016/j.tcm.2019.03.007 (2020).

23 Freda, B. J., Slawsky, M., Mallidi, J. & Braden, G. L. Decongestive treatment of acute decompensated heart failure: cardiorenal implications of ultrafiltration and diuretics. *Am J Kidney Dis* **58**, 1005-1017, doi:10.1053/j.ajkd.2011.07.023 (2011).

24 Vedin, O. *et al.* Significance of Ischemic Heart Disease in Patients With Heart Failure and Preserved, Midrange, and Reduced Ejection Fraction: A Nationwide Cohort Study. *Circ Heart Fail* **10**, doi:10.1161/circheartfailure.117.003875 (2017).

25 Gupta, A. *et al.* Association of the Hospital Readmissions Reduction Program Implementation With Readmission and Mortality Outcomes in Heart Failure. *JAMA Cardiol* **3**, 44-53, doi:10.1001/jamacardio.2017.4265 (2018).

26 Teerlink, J. R. *et al.* Effects of serelaxin in patients admitted for acute heart failure:

a meta-analysis. *European Journal of Heart Failure* **n/a**, doi:10.1002/ejhf.1692 (2019).

27 Chang, A. M. *et al.* Early Treatment in Emergency Department Patients with Acute Heart Failure: Does Time Matter? *Curr Heart Fail Rep* **16**, 12-20, doi:10.1007/s11897-019-0419-y (2019).

28 Bishu, K. *et al.* Biomarkers in acutely decompensated heart failure with preserved or reduced ejection fraction. *American heart journal* **164**, 763-770.e763, doi:10.1016/j.ahj.2012.08.014 (2012).

29 Bhuiyan, T. & Maurer, M. S. Heart Failure with Preserved Ejection Fraction: Persistent Diagnosis, Therapeutic Enigma. *Curr Cardiovasc Risk Rep* **5**, 440-449, doi:10.1007/s12170-011-0184-2 (2011).

30 Bredy, C. *et al.* New York Heart Association (NYHA) classification in adults with congenital heart disease: relation to objective measures of exercise and outcome. *Eur Heart J Qual Care Clin Outcomes* **4**, 51-58, doi:10.1093/ehjqcco/qcx031 (2018).

31 Filippatos, G. *et al.* Serelaxin in acute heart failure patients with preserved left ventricular ejection fraction: results from the RELAX-AHF trial. *Eur Heart J* **35**, 1041-1050, doi:10.1093/eurheartj/eht497 (2014).

32 Yancy, C. W., Lopatin, M., Stevenson, L. W., De Marco, T. & Fonarow, G. C. Clinical presentation, management, and in-hospital outcomes of patients admitted with acute decompensated heart failure with preserved systolic function: a report from the Acute Decompensated Heart Failure National Registry (ADHERE) Database. *J Am Coll Cardiol* **47**, 76-84, doi:10.1016/j.jacc.2005.09.022 (2006).

33 Sullivan, R. D., Mehta, R. M., Tripathi, R., Reed, G. L. & Gladysheva, I. P. Renin

Activity in Heart Failure with Reduced Systolic Function-New Insights. *Int J Mol Sci* **20**, 3182, doi:10.3390/ijms20133182 (2019).

34 Chang Patricia, P. *et al.* Trends in Hospitalizations and Survival of Acute Decompensated Heart Failure in Four US Communities (2005–2014). *Circulation* **138**, 12-24, doi:10.1161/CIRCULATIONAHA.117.027551 (2018).

35 van den Berge, J. C. *et al.* Left ventricular remodelling and prognosis after discharge in new-onset acute heart failure with reduced ejection fraction. *ESC Heart Fail*, doi:10.1002/ehf2.13299 (2021).

36 Schüttler, D., Clauss, S., Weckbach, L. T. & Brunner, S. Molecular Mechanisms of Cardiac Remodeling and Regeneration in Physical Exercise. *Cells* **8**, doi:10.3390/cells8101128 (2019).

37 Porter, K. E. & Turner, N. A. Cardiac fibroblasts: at the heart of myocardial remodeling. *Pharmacol Ther* **123**, 255-278, doi:10.1016/j.pharmthera.2009.05.002 (2009).

38 Azevedo, P. S., Polegato, B. F., Minicucci, M. F., Paiva, S. A. R. & Zornoff, L. A. M. Cardiac Remodeling: Concepts, Clinical Impact, Pathophysiological Mechanisms and Pharmacologic Treatment. *Arq Bras Cardiol* **106**, 62-69, doi:10.5935/abc.20160005 (2016).

39 Wu, Q.-Q. *et al.* Mechanisms contributing to cardiac remodelling. *Clinical Science* **131**, 2319-2345, doi:10.1042/CS20171167 (2017).

40 Sabbah, H. N. Pathophysiology of acute heart failure syndrome: a knowledge gap. *Heart Failure Reviews* **22**, 621-639, doi:10.1007/s10741-017-9651-2 (2017).

41 Collins, S. P. *et al.* What's Next for Acute Heart Failure Research? *Acad Emerg Med* **25**, 85-93, doi:10.1111/acem.13331 (2018).

42 Lattouf, R. *et al.* Picrosirius red staining: a useful tool to appraise collagen networks in normal and pathological tissues. *J Histochem Cytochem* **62**, 751-758, doi:10.1369/0022155414545787 (2014).

43 Banno, A. *et al.* Early vs. late reverse ventricular remodeling in patients with cardiomyopathy. *Journal of Cardiology* **68**, 57-63, doi:https://doi.org/10.1016/j.jjcc.2015.07.021 (2016).

44 Kubo, S. H. Neurohormonal activation and the response to converting enzyme inhibitors in congestive heart failure. *Circulation* **81**, Iii107-114 (1990).

45 Weber, K. T. *et al.* Fibrillar collagen and remodeling of dilated canine left ventricle. *Circulation* **82**, 1387-1401, doi:10.1161/01.cir.82.4.1387 (1990).

46 Sutton Martin, G. S. J. & Sharpe, N. Left Ventricular Remodeling After Myocardial Infarction. *Circulation* **101**, 2981-2988, doi:10.1161/01.CIR.101.25.2981 (2000).

47 Saavedra, W. F. *et al.* Reverse remodeling and enhanced adrenergic reserve from passive external support in experimental dilated heart failure. *J Am Coll Cardiol* **39**, 2069-2076, doi:10.1016/s0735-1097(02)01890-9 (2002).

48 Galli, A. & Lombardi, F. Postinfarct Left Ventricular Remodelling: A Prevailing Cause of Heart Failure. *Cardiology Research and Practice* **2016**, 2579832, doi:10.1155/2016/2579832 (2016).

49 Liu, G., Ma, C., Yang, H. & Zhang, P.-Y. Transforming growth factor β and its role in heart disease. *Exp Ther Med* **13**, 2123-2128, doi:10.3892/etm.2017.4246 (2017).

50 Wu, X. P., Wang, H. J., Wang, Y. L., Shen, H. R. & Tan, Y. Z. Serelaxin inhibits differentiation and fibrotic behaviors of cardiac fibroblasts by suppressing ALK-5/Smad2/3 signaling pathway. *Exp Cell Res* **362**, 17-27,

doi:10.1016/j.yexcr.2017.10.004 (2018).

51 Lapinskas, T. *et al.* Serelaxin Improves Regional Myocardial Function in Experimental Heart Failure: An In Vivo Cardiac Magnetic Resonance Study. *Journal of the American Heart Association* **9**, e013702, doi:10.1161/JAHA.119.013702 (2020).

52 Mukherji, A., Ansari, U., Borggrefe, M., Akin, I. & Behnes, M. Clinically Relevant Biomarkers in Acute Heart Failure: An Update. *Curr Pharm Biotechnol* **18**, 482-490, doi:10.2174/1389201018666170623090817 (2017).

53 Ali, D. & Banerjee, P. Inpatient Monitoring of Decompensated Heart Failure: What Is Needed? *Current Heart Failure Reports* **14**, 393-397, doi:10.1007/s11897-017-0352-x (2017).

54 Teerlink, J. R. *et al.* Serelaxin, recombinant human relaxin-2, for treatment of acute heart failure (RELAX-AHF): a randomised, placebo-controlled trial. *The Lancet* **381**, 29-39, doi:https://doi.org/10.1016/S0140-6736(12)61855-8 (2013).

55 Weintraub, N. L. *et al.* Acute heart failure syndromes: emergency department presentation, treatment, and disposition: current approaches and future aims: a scientific statement from the American Heart Association. *Circulation* **122**, 1975-1996, doi:10.1161/CIR.0b013e3181f9a223 (2010).

56 Teerlink, J. R. *et al.* Serelaxin in addition to standard therapy in acute heart failure: rationale and design of the RELAX-AHF-2 study. *Eur J Heart Fail* **19**, 800-809, doi:10.1002/ejhf.830 (2017).

57 Giam, B. *et al.* Serelaxin attenuates renal inflammation and fibrosis in a mouse model of dilated cardiomyopathy. *Exp Physiol* **103**, 1593-1602, doi:10.1113/ep087189 (2018).

58 Maggioni, A. P. *et al.* Efficacy and safety of serelaxin when added to standard of care in patients with acute heart failure: results from a PROBE study, RELAX-AHF-EU. *Eur J Heart Fail* **21**, 322-333, doi:10.1002/ejhf.1368 (2019).

59 Janssen, P. M. L. & Elnakish, M. T. Modeling heart failure in animal models for novel drug discovery and development. *Expert Opin Drug Discov* **14**, 355-363, doi:10.1080/17460441.2019.1582636 (2019).

60 Loungani, R. S. *et al.* Cause of Death in Patients With Acute Heart Failure: Insights From RELAX-AHF-2. *JACC Heart Fail* **8**, 999-1008, doi:10.1016/j.jchf.2020.09.010 (2020).

61 Lunney, M. *et al.* Pharmacological interventions for heart failure in people with chronic kidney disease. *Cochrane Database Syst Rev* **2**, Cd012466, doi:10.1002/14651858.CD012466.pub2 (2020).

62 Wilson, S. S., Ayaz, S. I. & Levy, P. D. Relaxin: A Novel Agent for the Treatment of Acute Heart Failure. *Pharmacotherapy: The Journal of Human Pharmacology and Drug Therapy* **35**, 315-327, doi:10.1002/phar.1548 (2015).

63 Jelinic, M. *et al.* Peptide hormone relaxin: from bench to bedside. *American Journal of Physiology-Regulatory, Integrative and Comparative Physiology* **314**, R753-R760, doi:10.1152/ajpregu.00276.2017 (2018).

64 Lam, M., Royce, S. G., Samuel, C. S. & Bourke, J. E. Serelaxin as a novel therapeutic opposing fibrosis and contraction in lung diseases. *Pharmacology & Therapeutics* **187**, 61-70, doi:https://doi.org/10.1016/j.pharmthera.2018.02.004 (2018).

65 Ponikowski, P. *et al.* Design of the RELAXin in acute heart failure study. *Am Heart J* **163**, 149-155.e141, doi:10.1016/j.ahj.2011.10.009 (2012).

66 Metra, M. *et al.* Effect of serelaxin on cardiac, renal, and hepatic biomarkers in the Relaxin in Acute Heart Failure (RELAX-AHF) development program: correlation with outcomes. *J Am Coll Cardiol* **61**, 196-206, doi:10.1016/j.jacc.2012.11.005 (2013).

67 Metra, M. *et al.* Effects of Serelaxin in Patients with Acute Heart Failure. *New England Journal of Medicine* **381**, 716-726, doi:10.1056/NEJMoa1801291 (2019).

68 Olivari, D. *et al.* Searching for Preclinical Models of Acute Decompensated Heart Failure: a Concise Narrative Overview and a Novel Swine Model. *Cardiovasc Drugs Ther*, doi:10.1007/s10557-020-07096-5 (2020).

69 Dixon, J. A. & Spinale, F. G. Large animal models of heart failure: a critical link in the translation of basic science to clinical practice. *Circ Heart Fail* **2**, 262-271, doi:10.1161/circheartfailure.108.814459 (2009).

70 Houser, S. R. *et al.* Animal models of heart failure: a scientific statement from the American Heart Association. *Circ Res* **111**, 131-150, doi:10.1161/RES.0b013e3182582523 (2012).

71 Nguyen, P. K. & Wu, J. C. Large Animal Models of Ischemic Cardiomyopathy: Are They Enough to Bridge the Translational Gap? *J Nucl Cardiol* **22**, 666-672, doi:10.1007/s12350-015-0078-7 (2015).

72 Silva, K. A. S. & Emter, C. A. Large Animal Models of Heart Failure: A Translational Bridge to Clinical Success. *JACC Basic Transl Sci* **5**, 840-856, doi:10.1016/j.jacbts.2020.04.011 (2020).

73 Rafael Clara, M., Mariana, P., Adelino, L.-M. & Paulo, C.-C. Relaxin and the Cardiovascular System: from Basic Science to Clinical Practice. *Current Molecular Medicine* **20**, 167-184,

doi:http://dx.doi.org/10.2174/1566524019666191023121607 (2020).

74 Dschietzig, T. *et al.* Intravenous recombinant human relaxin in compensated heart failure: a safety, tolerability, and pharmacodynamic trial. *J Card Fail* **15**, 182-190, doi:10.1016/j.cardfail.2009.01.008 (2009).

75 Jeyabalan, A., Shroff, S. G., Novak, J. & Conrad, K. P. The vascular actions of relaxin. *Adv Exp Med Biol* **612**, 65-87, doi:10.1007/978-0-387-74672-2_6 (2007).

76 Leo, C. H., Jelinic, M., Ng, H. H., Tare, M. & Parry, L. J. Time-dependent activation of prostacyclin and nitric oxide pathways during continuous i.v. infusion of serelaxin (recombinant human H2 relaxin). *Br J Pharmacol* **173**, 1005-1017, doi:10.1111/bph.13404 (2016).

77 Kanai, A. J., Konieczko, E. M., Bennett, R. G., Samuel, C. S. & Royce, S. G. Relaxin and fibrosis: Emerging targets, challenges, and future directions. *Molecular and Cellular Endocrinology* **487**, 66-74, doi:https://doi.org/10.1016/j.mce.2019.02.005 (2019).

78 Xu, M. M. *et al.* Serelaxin activates eNOS, suppresses inflammation, attenuates developmental delay and improves cognitive functions of neonatal rats after germinal matrix hemorrhage. *Sci Rep* **10**, 8115, doi:10.1038/s41598-020-65144-4 (2020).

79 Hettrick, D. A., Pagel, P. S. & Warltier, D. C. Desflurane, sevoflurane, and isoflurane impair canine left ventricular-arterial coupling and mechanical efficiency. *Anesthesiology* **85**, 403-413, doi:10.1097/00000542-199608000-00023 (1996).

80 Mannozzi, J. *et al.* Muscle metaboreflex-induced increases in effective arterial elastance: effect of heart failure. *Am J Physiol Regul Integr Comp Physiol* **319**, R1-r10, doi:10.1152/ajpregu.00040.2020 (2020).

81 Aragón-Herrera, A. *et al.* Serelaxin (recombinant human relaxin-2) treatment affects the endogenous synthesis of long chain poly-unsaturated fatty acids and induces substantial alterations of lipidome and metabolome profiles in rat cardiac tissue. *Pharmacol Res* **144**, 51-65, doi:10.1016/j.phrs.2019.04.009 (2019).

82 Bani, D. Recombinant human H2 relaxin (serelaxin) as a cardiovascular drug: aiming at the right target. *Drug Discov Today* **25**, 1239-1244, doi:10.1016/j.drudis.2020.04.014 (2020).

83 Dellavecchia, M. J. Inaccurate serelaxin chemical structure. *P T* **38**, 763-763 (2013).

84 Wilhelmi, T. *et al.* Serelaxin alleviates cardiac fibrosis through inhibiting endothelial-to-mesenchymal transition via RXFP1. *Theranostics* **10**, 3905-3924, doi:10.7150/thno.38640 (2020).

85 Shao, W., Rosales, C. B., Gonzalez, C., Prieto, M. C. & Navar, L. G. Effects of serelaxin on renal microcirculation in rats under control and high-angiotensin environments. *Am J Physiol Renal Physiol* **314**, F70-f80, doi:10.1152/ajprenal.00201.2017 (2018).

86 Sarwar, M., Du, X. J., Dschietzig, T. B. & Summers, R. J. The actions of relaxin on the human cardiovascular system. *Br J Pharmacol* **174**, 933-949, doi:10.1111/bph.13523 (2017).

87 Mordenti, J., Chen, S. A., Moore, J. A., Ferraiolo, B. L. & Green, J. D. Interspecies scaling of clearance and volume of distribution data for five therapeutic proteins. *Pharm Res* **8**, 1351-1359, doi:10.1023/a:1015836720294 (1991).

88 Neverova, N. & Teerlink, J. R. Serelaxin: a potential new drug for the treatment of acute heart failure. *Expert Opinion on Investigational Drugs* **23**, 1017-1026,

doi:10.1517/13543784.2014.924504 (2014).

89 Ghosh, R. K. *et al.* Serelaxin in acute heart failure: Most recent update on clinical and preclinical evidence. *Cardiovascular Therapeutics* **35**, 55-63, doi:10.1111/1755-5922.12231 (2017).

90 Snowdon, V. K. *et al.* Serelaxin as a potential treatment for renal dysfunction in cirrhosis: Preclinical evaluation and results of a randomized phase 2 trial. *PLoS Med* **14**, e1002248, doi:10.1371/journal.pmed.1002248 (2017).

91 Bøtker, H. E. *et al.* Practical guidelines for rigor and reproducibility in preclinical and clinical studies on cardioprotection. *Basic Res Cardiol* **113**, 39, doi:10.1007/s00395-018-0696-8 (2018).

92 Du, X. J., Hewitson, T. D., Nguyen, M. N. & Samuel, C. S. Therapeutic effects of serelaxin in acute heart failure. *Circ J* **78**, 542-552, doi:10.1253/circj.cj-14-0014 (2014).

93 Schiffner, R. *et al.* Altered Cerebral Blood Flow and Potential Neuroprotective Effect of Human Relaxin-2 (Serelaxin) During Hypoxia or Severe Hypovolemia in a Sheep Model. *Int J Mol Sci* **21**, doi:10.3390/ijms21051632 (2020).

94 Corallo, C. *et al.* Altered expression of RXFP1 receptor contributes to the inefficacy of relaxin-based anti-fibrotic treatments in systemic sclerosis. *Clin Exp Rheumatol* **37 Suppl 119**, 69-75 (2019).

95 Cáceres, F. T., Gaspari, T. A., Samuel, C. S. & Pinar, A. A. Serelaxin inhibits the profibrotic TGF-β1/IL-1β axis by targeting TLR-4 and the NLRP3 inflammasome in cardiac myofibroblasts. *The FASEB Journal* **33**, 14717-14733, doi:10.1096/fj.201901079RR (2019).

96 McCarthy, J. C. *et al.* Short-Term Administration of Serelaxin Produces

Predominantly Vascular Benefits in the Angiotensin II/L-NAME Chronic Heart Failure Model. *JACC Basic Transl Sci* **2**, 285-296, doi:10.1016/j.jacbts.2017.03.011 (2017).

97 Wang, D. *et al.* Serelaxin improves cardiac and renal function in DOCA-salt hypertensive rats. *Scientific Reports* **7**, 9793, doi:10.1038/s41598-017-09470-0 (2017).

98 Yu, L. *et al.* Serelaxin, recombinant human relaxin-2, for heart failure patients: A systematic review and meta-analysis. *Medicine (Baltimore)* **97**, e11010, doi:10.1097/md.0000000000011010 (2018).

99 Harjola, V.-P. *et al.* Organ dysfunction, injury and failure in acute heart failure: from pathophysiology to diagnosis and management. A review on behalf of the Acute Heart Failure Committee of the Heart Failure Association (HFA) of the European Society of Cardiology (ESC). *European Journal of Heart Failure* **19**, 821-836, doi:10.1002/ejhf.872 (2017).

100 Verhulst, A., Neven, E. & D'Haese, P. C. Characterization of an Animal Model to Study Risk Factors and New Therapies for the Cardiorenal Syndrome, a Major Health Issue in Our Aging Population. *Cardiorenal Medicine* **7**, 234-244, doi:10.1159/000462984 (2017).

101 Lindsey, M. L. *et al.* Guidelines for experimental models of myocardial ischemia and infarction. *Am J Physiol Heart Circ Physiol* **314**, H812-h838, doi:10.1152/ajpheart.00335.2017 (2018).

102 Unemori, E. Serelaxin in clinical development: past, present and future. *Br J Pharmacol* **174**, 921-932, doi:10.1111/bph.13695 (2017).

103 Chow Sheryl, L. *et al.* Role of Biomarkers for the Prevention, Assessment, and

Management of Heart Failure: A Scientific Statement From the American Heart Association. *Circulation* **135**, e1054-e1091, doi:10.1161/CIR.0000000000000490 (2017).

104 Powers, J. C. Canine Model of Pacing-Induced Heart Failure. *Methods in molecular biology (Clifton, N.J.)* **1816**, 309-325, doi:10.1007/978-1-4939-8597-5_24 (2018).

105 Sabbah, H. N. *et al.* A canine model of chronic heart failure produced by multiple sequential coronary microembolizations. *American Journal of Physiology-Heart and Circulatory Physiology* **260**, H1379-H1384, doi:10.1152/ajpheart.1991.260.4.H1379 (1991).

106 Dunlay, S. M. & Roger, V. L. Understanding the Epidemic of Heart Failure: Past, Present, and Future. *Current Heart Failure Reports* **11**, 404-415, doi:10.1007/s11897-014-0220-x (2014).

107 Heidenreich, P. A. *et al.* Forecasting the Impact of Heart Failure in the United States: A Policy Statement From the American Heart Association. *Circulation. Heart failure* **6**, 606-619, doi:10.1161/HHF.0b013e318291329a (2013).

108 Hardin, E. A. & Grodin, J. L. Diuretic Strategies in Acute Decompensated Heart Failure. *Curr Heart Fail Rep* **14**, 127-133, doi:10.1007/s11897-017-0319-y (2017).

109 Houser, S. R. *et al.* Animal Models of Heart Failure. *A Scientific Statement From the American Heart Association* **111**, 131-150, doi:10.1161/RES.0b013e3182582523 (2012).

110 Monnet, E. & Chachques, J. C. Animal Models of Heart Failure: What Is New? *The Annals of Thoracic Surgery* **79**, 1445-1453, doi:http://dx.doi.org/10.1016/j.athoracsur.2004.04.002 (2005).

111 Nguyen, P. K. & Wu, J. C. Large Animal Models of Ischemic Cardiomyopathy: Are They Enough to Bridge the Translational Gap? *Journal of Nuclear Cardiology* **22**, 666-672, doi:10.1007/s12350-015-0078-7 (2015).

112 Recchia, F. A. & Lionetti, V. Animal Models of Dilated Cardiomyopathy for Translational Research. *Veterinary Research Communications* **31**, 35-41, doi:10.1007/s11259-007-0005-8 (2007).

113 Schmitto, J. D. *et al.* Large Animal Models of Chronic Heart Failure (CHF). *Journal of Surgical Research* **166**, 131-137, doi:http://dx.doi.org/10.1016/j.jss.2009.11.737 (2011).

114 Maxwell, M. P., Hearse, D. J. & Yellon, D. M. Species variation in the coronary collateral circulation during regional myocardial ischaemia: a critical determinant of the rate of evolution and extent of myocardial infarction. *Cardiovasc Res* **21**, 737-746, doi:10.1093/cvr/21.10.737 (1987).

115 Weaver, M. E., Pantely, G. A., Bristow, J. D. & Ladley, H. D. A quantitative study of the anatomy and distribution of coronary arteries in swine in comparison with other animals and man. *Cardiovasc Res* **20**, 907-917, doi:10.1093/cvr/20.12.907 (1986).

116 Roos, A. & Smith, J. R. Production of experimental heart failure in dogs with intact circulation. *Am J Physiol* **153**, 558-566, doi:10.1152/ajplegacy.1948.153.3.558 (1948).

117 Morita, H. *et al.* Selective matrix metalloproteinase inhibition attenuates progression of left ventricular dysfunction and remodeling in dogs with chronic heart failure. *American Journal of Physiology - Heart and Circulatory Physiology* **290**, H2522-H2527, doi:10.1152/ajpheart.00932.2005 (2006).

118 Saavedra, W. F. *et al.* Reverse remodeling and enhancedadrenergic reserve from passive externalsupport in experimental dilated heart failure. *Journal of the American College of Cardiology* **39**, 2069-2076, doi:http://doi.org/10.1016/S0735-1097(02)01890-9 (2002).

119 Sabbah, H. N. *et al.* A canine model of chronic heart failure produced by multiple sequential coronary microembolizations. *American Journal of Physiology - Heart and Circulatory Physiology* **260**, H1379-H1384 (1991).

120 Smiseth, O. A. PROGRESSION OF MYOCARDIAL DAMAGE FOLLOWING CORONARY MICROEMBOLIZATION IN DOGS. *Acta pathologica, microbiologica et immunologica Scandinavica. Section A. Pathology* **91A**, 115-124.

121 Todaka, K. *et al.* Characterizing ventricular mechanics and energetics following repeated coronary microembolization. *Am J Physiol* **272**, H186-194, doi:10.1152/ajpheart.1997.272.1.H186 (1997).

122 Heusch, G. *et al.* Coronary Microembolization. *From Bedside to Bench and Back to Bedside* **120**, 1822-1836, doi:10.1161/circulationaha.109.888784 (2009).

123 Lavine, S. J., Prcevski, P., Held, A. C. & Johnson, V. Experimental model of chronic global left ventricular dysfunction secondary to left coronary microembolization. *Journal of the American College of Cardiology* **18**, 1794-1803, doi:http://dx.doi.org/10.1016/0735-1097(91)90523-C (1991).

124 Hasenfuss, G. Animal models of human cardiovascular disease, heart failure and hypertrophy. *Cardiovascular research* **39**, 60-76 (1998).

125 Unverferth, D. V. *et al.* The evolution of beta-adrenergic dysfunction during the induction of canine cobalt cardiomyopathy. *Cardiovasc Res* **18**, 44-50, doi:10.1093/cvr/18.1.44 (1984).

126 Armstrong, P. W., Stopps, T. P., Ford, S. E. & de Bold, A. J. Rapid ventricular pacing in the dog: pathophysiologic studies of heart failure. *Circulation* **74**, 1075-1084, doi:10.1161/01.cir.74.5.1075 (1986).

127 Burkett, D. E. *et al.* Myocardial effects of repetitive episodes of rapid ventricular pacing in conscious dogs: surgical creation, echocardiographic evaluation, and morphometric analysis. *Lab Anim Sci* **44**, 453-461 (1994).

128 Hammond, R. L. *et al.* Heart failure alters the strength and mechanisms of the muscle metaboreflex. *American Journal of Physiology - Heart and Circulatory Physiology* **278**, H818-H828 (2000).

129 O'Rourke, B. *et al.* Mechanisms of Altered Excitation-Contraction Coupling in Canine Tachycardia-Induced Heart Failure, I. *Experimental Studies* **84**, 562-570, doi:10.1161/01.res.84.5.562 (1999).

130 Weber, K. T. *et al.* Fibrillar collagen and remodeling of dilated canine left ventricle. *Circulation* **82**, 1387-1401, doi:10.1161/01.cir.82.4.1387 (1990).

131 Mannozzi, J., Massoud, L., Kaur, J., Coutsos, M. & O'Leary, D. S. Ventricular contraction and relaxation rates during muscle metaboreflex activation in heart failure: are they coupled? *Exp Physiol* **106**, 401-411, doi:10.1113/ep089053 (2021).

132 Augustyniak, R. A. *et al.* Cardiovascular responses to exercise and muscle metaboreflex activation during the recovery from pacing-induced heart failure. *J Appl Physiol (1985)* **101**, 14-22, doi:10.1152/japplphysiol.00072.2006 (2006).

133 Bosch, L. *et al.* The transverse aortic constriction heart failure animal model: a systematic review and meta-analysis. *Heart Fail Rev*, doi:10.1007/s10741-020-09960-w (2020).

134 Hittinger, L. *et al.* Isoproterenol-induced alterations in myocardial blood flow, systolic and diastolic function in conscious dogs with heart failure. *Circulation* **80**, 658-668, doi:10.1161/01.cir.80.3.658 (1989).

135 Lerman, L. O., Chade, A. R., Sica, V. & Napoli, C. Animal models of hypertension: An overview. *Journal of Laboratory and Clinical Medicine* **146**, 160-173, doi:https://doi.org/10.1016/j.lab.2005.05.005 (2005).

136 Morioka, S. & Simon, G. Echocardiographic evidence for early left ventricular hypertrophy in dogs with renal hypertension. *The American Journal of Cardiology* **49**, 1890-1895, doi:http://dx.doi.org/10.1016/0002-9149(82)90207-7 (1982).

137 Sarikonda, K. V., Watson, R. E., Opara, O. C. & DiPette, D. J. Experimental animal models of hypertension. *Journal of the American Society of Hypertension* **3**, 158-165, doi:http://doi.org/10.1016/j.jash.2009.02.003 (2009).

138 McKie, P. M. *et al.* M-Atrial Natriuretic Peptide and Nitroglycerin in a Canine Model of Experimental Acute Hypertensive Heart Failure: Differential Actions of 2 cGMP Activating Therapeutics. *Journal of the American Heart Association: Cardiovascular and Cerebrovascular Disease* **3**, e000206, doi:10.1161/JAHA.113.000206 (2014).

139 Bristow, M. R. *et al.* Acute and chronic cardiovascular effects of doxorubicin in the dog: the cardiovascular pharmacology of drug-induced histamine release. *J Cardiovasc Pharmacol* **2**, 487-515, doi:10.1097/00005344-198009000-00002 (1980).

140 Monnet, E. & Christopher Orton, E. A canine model of heart failure by intracoronary adriamycin injection: Hemodynamic and energetic results. *Journal of Cardiac Failure* **5**, 255-264, doi:http://dx.doi.org/10.1016/S1071-9164(99)90010-6 (1999).

141 Toyoda, Y., Okada, M. & Kashem, M. A. A canine model of dilated cardiomyopathy induced by repetitive intracoronary doxorubicin administration. *The Journal of Thoracic and Cardiovascular Surgery* **115**, 1367-1373, doi:http://doi.org/10.1016/S0022-5223(98)70221-1 (1998).

142 Arnold, J. M. O. *et al.* Differential effects of reperfusion on incidence of ventricular arrhythmias and recovery of ventricular function at 4 days following coronary occlusion. *American Heart Journal* **113**, 1055-1065, doi:http://dx.doi.org/10.1016/0002-8703(87)90912-4 (1987).

143 Jugdutt, B. I. & Menon, V. Valsartan-induced cardioprotection involves angiotensin II type 2 receptor upregulation in dog and rat models of in vivo reperfused myocardial infarction. *Journal of Cardiac Failure* **10**, 74-82, doi:http://doi.org/10.1016/S1071-9164(03)00584-0 (2004).

144 Deedwania, P. C. & Lardizabal, J. A. Atrial Fibrillation in Heart Failure: A Comprehensive Review. *The American Journal of Medicine* **123**, 198-204, doi:https://doi.org/10.1016/j.amjmed.2009.06.033 (2010).

145 Kaur J, K. A. Altered arterial baroreflex-muscle metaboreflex interaction in heart failure. *Am J Physiol Heart Circ Physiol.* **315** (2018).

146 Sabbah, H. N. *et al.* A canine model of chronic heart failure produced by multiple sequential coronary microembolizations. *Am J Physiol* **260**, H1379-1384, doi:10.1152/ajpheart.1991.260.4.H1379 (1991).

147 van der Meer, P., Gaggin, H. K. & Dec, G. W. ACC/AHA Versus ESC Guidelines on Heart Failure: JACC Guideline Comparison. *J Am Coll Cardiol* **73**, 2756-2768, doi:10.1016/j.jacc.2019.03.478 (2019).

148 Sondeen, J. L. & Claybaugh, J. R. Clearance and urinary excretion of vasopressin

in conscious dogs. *American Journal of Physiology - Regulatory, Integrative and Comparative Physiology* **256**, R291-R298 (1989).

149 Bivona, B. J., Park, S. & Harrison-Bernard, L. M. Glomerular filtration rate determinations in conscious type II diabetic mice. *American Journal of Physiology-Renal Physiology* **300**, F618-F625, doi:10.1152/ajprenal.00421.2010 (2011).

150 Sondeen, J. L. & Claybaugh, J. R. Clearance and urinary excretion of vasopressin in conscious dogs. *Am J Physiol* **256**, R291-298, doi:10.1152/ajpregu.1989.256.2.R291 (1989).

151 Smiseth, O. A., Lindal, S., Mjøs, O. D., Vik-Mo, H. & Jørgensen, L. Progression of myocardial damage following coronary microembolization in dogs. *Acta Pathol Microbiol Immunol Scand A* **91**, 115-124, doi:10.1111/j.1699-0463.1983.tb02735.x (1983).

152 Wang, M. *et al.* Acute Intravenous Infusion of an Adenosine Regulating Agent Improves Left Ventricular Function in Dogs with Advanced Heart Failure. *Cardiovascular Drugs and Therapy* **27**, 489-498, doi:10.1007/s10557-013-6482-9 (2013).

153 Packer, M. Why Are Physicians So Confused about Acute Heart Failure? *New England Journal of Medicine* **381**, 776-777, doi:10.1056/NEJMe1904713 (2019).

154 Kass, D. A. Age-related changes in venticular-arterial coupling: pathophysiologic implications. *Heart Fail Rev* **7**, 51-62, doi:10.1023/a:1013749806227 (2002).

155 Kass David, A. Ventricular Arterial Stiffening. *Hypertension* **46**, 185-193, doi:10.1161/01.HYP.0000168053.34306.d4 (2005).

156 Kingwell, B. A. Large artery stiffness: implications for exercise capacity and cardiovascular risk. *Clin Exp Pharmacol Physiol* **29**, 214-217, doi:10.1046/j.1440-

1681.2002.03622.x (2002).

157 Cáceres, F. T., Gaspari, T. A., Samuel, C. S. & Pinar, A. A. Serelaxin inhibits the profibrotic TGF-β1/IL-1β axis by targeting TLR-4 and the NLRP3 inflammasome in cardiac myofibroblasts. *Faseb j* **33**, 14717-14733, doi:10.1096/fj.201901079RR (2019).

158 Samuel, C. S. *et al.* Anti-fibrotic actions of relaxin. *Br J Pharmacol* **174**, 962-976, doi:10.1111/bph.13529 (2017).

159 Kaur, J. *et al.* Altered arterial baroreflex-muscle metaboreflex interaction in heart failure. *Am J Physiol Heart Circ Physiol* **315**, H1383-H1392, doi:10.1152/ajpheart.00338.2018 (2018).

160 Fincke, R. *et al.* Cardiac power is the strongest hemodynamic correlate of mortality in cardiogenic shock: A report from the SHOCK trial registry. *Journal of the American College of Cardiology* **44**, 340 (2004).

161 Fincke, R. *et al.* Cardiac power is the strongest hemodynamic correlate of mortality in cardiogenic shock: A report from the SHOCK trial registry. *Journal of the American College of Cardiology* **44**, 340-348, doi:https://doi.org/10.1016/j.jacc.2004.03.060 (2004).

162 Bivona, B. J., Park, S. & Harrison-Bernard, L. M. Glomerular filtration rate determinations in conscious type II diabetic mice. *American Journal of Physiology-Renal Physiology* **300**, F618-F625, doi:10.1152/ajprenal.00421.2010 (2010).

163 Waldman, B. M., Augustyniak, R. A., Chen, H. & Rossi, N. F. Effects of voluntary exercise on blood pressure, angiotensin II, aldosterone, and renal function in two-kidney, one-clip hypertensive rats. *Integr Blood Press Control* **10**, 41-51, doi:10.2147/ibpc.S147122 (2017).

164 Feng, H. Z., Biesiadecki, B. J., Yu, Z. B., Hossain, M. M. & Jin, J. P. Restricted N-terminal truncation of cardiac troponin T: a novel mechanism for functional adaptation to energetic crisis. *J Physiol* **586**, 3537-3550, doi:10.1113/jphysiol.2008.153577 (2008).

165 Feng, H. Z., Chen, X., Malek, M. H. & Jin, J. P. Slow recovery of the impaired fatigue resistance in postunloading mouse soleus muscle corresponding to decreased mitochondrial function and a compensatory increase in type I slow fibers. *Am J Physiol Cell Physiol* **310**, C27-40, doi:10.1152/ajpcell.00173.2015 (2016).

166 Mukherji, A. Clinically Relevant Biomarkers in Acute Heart Failure: An Update. *Current pharmaceutical biotechnology* **18**, 482-490, doi:10.2174/1389201018666170623090817 (2017).

167 Burgos, L. M. *et al.* Does high sensitivity troponin add prognostic value to validated risk scores to predict in-hospital mortality in patients with acute heart failure? *Heart Vessels*, doi:10.1007/s00380-021-01847-6 (2021).

168 Heusch, G. *et al.* Coronary microembolization: from bedside to bench and back to bedside. *Circulation* **120**, 1822-1836, doi:10.1161/circulationaha.109.888784 (2009).

169 Komamura, K. *et al.* Alterations in left ventricular diastolic function in conscious dogs with pacing-induced heart failure. *J Clin Invest* **89**, 1825-1838, doi:10.1172/JCI115787 (1992).

170 Valle Raleigh, J. *et al.* Reperfusion therapy with recombinant human relaxin-2 (Serelaxin) attenuates myocardial infarct size and NLRP3 inflammasome following ischemia/reperfusion injury via eNOS-dependent mechanism. *Cardiovasc Res*

113, 609-619, doi:10.1093/cvr/cvw246 (2017).

171 Wang, D. *et al.* Serelaxin improves cardiac and renal function in DOCA-salt hypertensive rats. *Sci Rep* **7**, 9793-9793, doi:10.1038/s41598-017-09470-0 (2017).

172 Flameng, W., Schwarz, F. & Schaper, W. Coronary collaterals in the canine heart: development and functional significance. *American Heart Journal* **97**, 70-77, doi:https://doi.org/10.1016/0002-8703(79)90116-9 (1979).

173 Wang, M. *et al.* Acute intravenous infusion of an adenosine regulating agent improves left ventricular function in dogs with advanced heart failure. *Cardiovasc Drugs Ther* **27**, 489-498, doi:10.1007/s10557-013-6482-9 (2013).

174 Foo, J. Y. *et al.* Circulating fragments of N-terminal pro-B-type natriuretic peptides in plasma of heart failure patients. *Clin Chem* **59**, 1523-1531, doi:10.1373/clinchem.2012.200204 (2013).

175 Bosch, X., Poch, E. & Grau, J. M. Rhabdomyolysis and acute kidney injury. *N Engl J Med* **361**, 62-72, doi:10.1056/NEJMra0801327 (2009).

176 Collins, S. P. *et al.* Feasibility of Serial 6-min Walk Tests in Patients with Acute Heart Failure. *J Clin Med* **6**, doi:10.3390/jcm6090084 (2017).

177 Matthews, S., Levy, P. D., Favot, M., Gowland, L. & Abidov, A. Three-dimensional echocardiography in acute heart failure: Can and should we do it in the emergency department? *Echocardiography* **35**, 692-694, doi:10.1111/echo.14011 (2018).

178 Sun, J. *et al.* Human Relaxin-2 Fusion Protein Treatment Prevents and Reverses Isoproterenol-Induced Hypertrophy and Fibrosis in Mouse Heart. *Journal of the American Heart Association* **8**, e013465-e013465, doi:10.1161/JAHA.119.013465 (2019).

179 Varvodic, J. *et al.* Trying to Survive A Serious Heart Condition in Time of COVID-19. *Heart Surg Forum* **24**, E372-e374, doi:10.1532/hsf.3815 (2021).

ABSTRACT

DECIPHERING THE CARDIORENAL EFFECTS OF SERELAXIN IN ACUTE HEART FAILURE- A CANINE MODEL

by

ABHINAV C. KRISHNAN

August 2021

Advisor: Dr. Phillip D. Levy

Major: Physiology

Degree: Doctor of Philosophy

Acute heart failure (HF) with underlying ischemic cardiomyopathy (ICM) is one of the leading causes of cardiovascular associated death in the United States. Acute HF pathophysiology involves a complex interplay of neurohormonal activation, increased cardiac ventricular pressures (fluid overload), vasoconstriction, impaired renal function, and progressive end-organ failure. Serelaxin (SLX), a recombinant form of the human hormone relaxin 2, is a vasodilator and an ideal pharmacological agent to treat acute HF. Though SLX was associated with positive preliminary outcome data for acute HF it however failed to provide benefit during clinical trials. Greater understanding of cardiac and renal parameters may elucidate these neutral findings.

We addressed two specific questions: 1) To what extent does SLX treatment of acute HF with underlying ICM improve cardiac associated hemodynamics and biomarkers 2) To what extent does SLX treatment of acute HF with underlying ICM improve renal associated hemodynamics and biomarkers. Our study utilized a novel, highly translatable canine model of acute-on-chronic heart failure, data were collected before and after the induction of ICM, following acute HF, and during and after SLX/placebo treatment over

30 days. We found 1) SLX does not significantly improve acute HF blunted cardiac hemodynamics or biomarkers, 30 days post-treatment vs placebo. 2) Acute HF blunted renal hemodynamics and biomarkers were not significantly improved following SLX treatment vs placebo. As such, SLX did not significantly improve acute HF associated cardiac and renal hemodynamics, which further parallels the finds of the human RELAX-AHF2 clinical trial results that show little to no significant improvement in SLX in improving acute HF-linked parameters and outcomes.

AUTOBIOGRAPHICAL STATEMENT

ABHINAV C. KRISHNAN

Education

2018–2021	**Ph.D., Physiology** Wayne State University School of Medicine, Detroit, MI
2017–2019	**BC-PHP, Public Health** Wayne State University, Detroit, MI
2014–2017	**M.S., Physiology** Wayne State University School of Medicine, Detroit, MI
2006–2011	**B.S., Secondary Education & B.S., Biological Sciences** Wayne State University, Detroit, MI

Publications

1. Stewart B, Brody A, **Krishnan AC**, Brown SK, Levy PD. "An Unmet Need Meets an Untapped Resource: Pharmacist-Led Pthways for Hypertension Management for Emergency Department Patients" Curr Hypertens Rep. **2019 Jun 19**. Doi 10.1007/s11906-019-0965-4.
2. Kaur J, **Krishnan AC**, Senador D, Alvarez A, Hanna HW, O'Leary DS. "Altered Arterial Baroreflex – Muscle Metaboreflex Interaction in Heart Failure". Am J Physiol Heart Circ Physiol. **2018 Aug 3**. doi: 10.1152/ajpheart.00338.2018. [Epub ahead of print]
3. Kaur J, Senador D, **Krishnan AC**, Hanna HW, Alvarez A, Machado TM, O'Leary DS. "Muscle Metaboreflex-Induced Vasoconstriction in the Ischemic Active Muscle is Exaggerated in Heart Failure". Am J Physiol Heart Circ Physiol. **2017 Sep 22**: ajpheart.00375.2017. doi: 10.1152/ajpheart.00375.2017. [Epub ahead of print]
4. Spranger MD, Kaur J, Sala-Mercado JA, **Krishnan AC**, Abu-Hamdah R, Alvarez A, Machado TM, Augustyniak RA, O'Leary DS. "*Exaggerated coronary vasoconstriction limits muscle metaboreflex-induced increases in ventricular performance in hypertension*". Am J Physiol Heart Circ Physiol. **2017 Jan 1**;312(1):H68-H79. doi: 10.1152/ajpheart.00417.2016.
5. Spranger MD, Kaur J, Sala-Mercado JA, **Krishnan AC**, Abu-Hamdah R, Alvarez A, Machado TM, Augustyniak RA, O'Leary DS. "*Exaggerated coronary vasoconstriction limits muscle metaboreflex-induced increases in ventricular performance in hypertension*". Am J Physiol Heart Circ Physiol. **2017 Jan 1**;312(1):H68-H79. doi: 10.1152/ajpheart.00417.2016.
6. Kaur J, Alvarez A, Hanna HW, **Krishnan AC**, Senador D, Machado TM, Altamimi YH, Lovelace A, Dombrowski M, Spranger MD, O'Leary DS. "*Interaction between the Muscle Metaboreflex and Arterial Baroreflex in the Control of Arterial Pressure and Skeletal Muscle Blood Flow*". Am J Physiol Heart Circ Physiol. **2016 Nov 1**;311(5):H1268-H1276. doi: 10.1152/ajpheart.00501.2016
7. Spranger MD, **Krishnan AC,** Levy PD, O'Leary DS, Smith SA. *"Reply to "Letter to the editor: Applying the blood flow restriction pressure: the elephant in the room".* Am J Physiol Heart Circ Physiol. **2016 Jan 1**;310(1):H134-5. doi:10.1152/ajpheart.00878.2015.
8. Kaur J, Machado TM, Alvarez A, **Krishnan AC**, Hanna HW, Altamimi YH, Senador D, Spranger MD, O'Leary DS. "*Muscle Metaboreflex Activation during Dynamic Exercise Vasoconstricts the Ischemic Active Skeletal Muscle*". Am J Physiol Heart Circ Physiol. **2015 Dec 15**;309(12):H2145-51. doi: 10.1152/ajpheart.00679.2015. Epub 2015 Oct 16.
9. Spranger MD, **Krishnan AC,** Levy PD, O'Leary DS, Smith SA. *"Blood flow restriction training and the exercise pressor reflex: a call for concern*". Am J Physiol Heart Circ Physiol. **2015 Nov**;309(9):H1440-52. doi: 10.1152/ajpheart.00208.2015. Epub 2015 Sep 4. Review.
10. Spranger MD, Kaur J, Sala-Mercado JA, Machado TM, **Krishnan AC**, Alvarez A, O'Leary DS. "Attenuated muscle metaboreflex-induced pressor response during post-exercise muscle ischemia in renovascular hypertension". Am J Physiol Regul Integr Comp Physiol. **2015 Apr 1**; 308(7): R650-8. doi: 10.1152/ajpregu.00464.2014. Epub 2015 Jan 28.
11. Kaur J, Spranger MD, Hammond RL, **Krishnan AC,** Alvarez A, Augustyniak RA, O'Leary DS. "*Muscle metaboreflex activation during dynamic exercise evokes epinephrine release resulting in β2-mediated vasodilation".* Am J Physiol Heart Circ Physiol. **2015 Mar 1**;308(5):H524-9. doi: 10.1152/ajpheart.00648.2014. Epub 2014 Dec 24.